Optimization of multiple-crane service schedules in overlapping areas through consideration of transportation efficiency and operational safety

Chun Huang[1,2], Wenjie Li[1,2], Weisheng Lu[3], Fan Xue [3], Meng Liu[1,2], Zhansheng Liu[1,2*]

[1] College of Architecture and Civil Engineering, Beijing University of Technology, Chaoyang, Beijing 100124, China
[2] The Key Laboratory of Urban Security and Disaster Engineering of the Ministry of Education, Beijing University of Technology, Beijing 100124, China
[3] Department of Real Estate and Construction, Faculty of Architecture, The University of Hong Kong, Pokfulam, Hong Kong SAR, China
*Corresponding author: Email: lzs4216@163.com

This is the peer-reviewed post-print version of the paper:

Huang, C., Li, W., Lu, W., Xue, F., Liu, M., & Liu, Z. (2021). Optimization of multiple-crane service schedules in overlapping areas through consideration of transportation efficiency and operational safety. *Automation in Construction*, 127, 103716. Doi: 10.1016/j.autcon.2021.103716

The final version of this paper is available at: https://doi.org/10.1016/j.autcon.2021.103716.

Abstract

Tower crane scheduling is a classic conundrum. It is further complicated to prevent collisions and reduce idle transportation time among multiple overlapping tower cranes. Unlike previous research attempts, this study aims to provide an optimal solution to this multiple crane service scheduling problem (MCSSP). Firstly, the MCSSP was translated to a Mixed Integer Linear Programming (MILP) model. Then, the model was optimized by 1) distributing the lifting requests in overlapping areas to the proper tower cranes; 2) selecting the appropriate supply location to serve each lifting request; and 3) arranging the lifting sequences of each tower crane to complete the requests. Compared with previous methods, the proposed MILP model (solved using Gurobi™) can result in the saving of 6.54%-18.07% of total operation costs meanwhile achieving the non-collision goal. The findings of this research can be deployed in optimizing efficiency and safety in the real-life scheduling of multiple overlapping tower cranes.

Keywords: multiple tower cranes; service schedule optimization; overlapping site areas; transportation efficiency; collision free.

1. Introduction

Tower cranes are used to transport equipment and material on site and are thus some of the most essential facilities in contemporary construction work. When multiple tower cranes are deployed on site, the working radius of each crane is determined. For each pair of tower cranes, if the distance between the cranes is smaller than the sum of the two radius, and larger than the absolute value of the difference between the two radius, then there is an area of overlap between the two cranes. This sort of overlap is inevitable when a site area is limited or the high lifting workload in a working area requires simultaneous crane operations. Such overlaps, however, mean that crane collisions become a potential hazard. Tower crane jibs are liable to collide with the jibs or cables of other cranes, regardless of the cranes' different heights [1]. Irizarry and Karan [2] developed a system for minimizing areas of overlap but were not able to entirely remove the possibility of physical conflicts between cranes [3, 4]. On any site with overlapping cranes, therefore, crane-related lift planning and optimization (LPO) is a very critical task for planners so as to ensure operational efficiency and safety [5].

In practice, starting location and destination for each crane operation are always pre-scheduled based on the material requests. Having an efficient service schedule helps to prevent situations in which crane movements in overlapping areas are disturbed at random intervals by the movements of other tower cranes [6]. To prevent potential collisions, tower cranes make use of anti-collision systems. These consist of various sensors and devices, such as Ultra-Wide Band (UWB) [1, 7], Radio Frequency Identifications (RFID) [8, 9], Global Positioning System (GPS) [7-9], Encoder [10, 11], and Inertial Measurement Unit (IMU) [10-12] to measure distances between moving jibs and their surroundings. When the distance is too close and a collision becomes imminent, the anti-collision system will trigger an alarm and slow down or stop the moving jibs. However, negatively suspending crane movements or tuning their velocity can have a significant and negative impact on transportation efficiency. Site managers have expressed doubts about the usefulness of anti-collision systems, as these have been known to cause unnecessary stoppages and slow down work schedules.

Preventing crane collisions in overlapping areas at the same time as reducing idle transportation time presents a difficult conundrum. To solve this conundrum, the present research systematically studied the service schedules of multiple cranes. By determining starting locations and destinations for each crane operation service schedules can have a significant impact on improving transportation efficiency. For a single crane, devising effective linkages among material requests and the locations of cranes and storage areas has been demonstrated to guarantee a high ratio of crane utilization [13]. For multiple tower cranes, this research proposed an MILP model to optimize service schedules in a way that allows for the completing of lifting tasks with minimum energy costs. To avoid collisions in overlapping areas, simultaneous movements are forbidden in these areas. A crane is only permitted to enter an overlapping area after the other crane has moved out. Previous research has simulated the interactions between requests, cranes and supply points and has succeeded in proposing operational methods that eliminate simultaneous movements in overlapping areas [3, 14]. However, while this research has enhanced crane operations within the parameters of acceptable schedules, the simulations fail to lead to fully optimized results [3]. Formulated according to different linear constraints, the MILP model proposed in the present paper, on the other hand, is able to guarantee both operational safety and a method for ensuring optimally efficient service schedules.

Following this introductory section, the literature review in Section 2 provides an overview of existing techniques and methods in the study of crane operation safety and efficiency. Section 3 presents the problem statement and the assumptions of the proposed model. Section 4 explains the objective function and the linear constraints of the optimization model. Section 5 details the application of the model in numerical studies and compares the results of different methods to demonstrate the effectiveness of the model. Section 6 provides a summary of findings, draws conclusions and outlines the various contributions and limitations of this research.

2. Literature review

In general, there are three principal aspects that can significantly affect the efficiency and safety of tower crane operations: (i) the selection and layout of tower cranes on construction sites; (ii) lifting path and motion planning; and (iii) the lifting schedule of each tower crane. During the preconstruction stage, the deployment of the proper types and quantities of tower cranes at appropriate locations can achieve sufficient on-site coverage for the conducting of safe and efficient operations. Location optimization studies account for the largest proportion of research into crane-related LPO [5]. The optimization algorithms and simulation methods used to solve the problem in previous research include Genetic Algorithm (GA) [15-17], Mixed-Integer-Programming (MIP) [18-22], Agent-Based Simulation (ABS) [23] and Simulated Annealing (SA) [24]. Visualization tools such as CAD and BIM have also been profitably employed to assist in crane layout planning [2, 25, 26].

To study lifting path planning in a simulated environment, the cranes are simulated as 3D virtual kinematical models by assigning different degrees-of-freedom (DOF) [27, 28]. The accuracy and efficiency of searches aimed at identifying the shortest and collision-free paths are highly dependent on the representations of space and objects and the searching algorithm. Configuration space (C-Space), in which each axis denotes a DOF, is widely used to represent space without redundancy [29]. To prevent penetrations between objects, objects in complex geometric shapes can be wrapped by hierarchical bounding volumes such as Axis-aligned Bounding Box (AABB) [30], Oriented Bounding Box (OBB) [31] and Spheres [32]. Avoiding the overlap of the objects intervals along each axis, the searching algorithms used to search optimal lifting paths include GA [33], Rapidly-exploring Random Tree (RRT) [34] and Probabilistic Road Map (PRM) [35]. The principal concern when path planning is to accelerate the searching process and improve efficiency. There have been pre-calculations proposed in previous research that attempt to reduce the feasible C-space [33, 35, 36]. Based on Multi-level Depth Map (MDM) representation, Cai et al. [37] proposed an image-space parallel collision detection algorithm and simplified a Master-Slave Parallel Genetic Algorithm (MSPGA) by using parallel threads in a Graphics Processing Unit (GPU). To avoid obstacles in a dynamic environment, computer vision algorithms and laser scanners [10] have been used to identify and track the real-time locations of crane components [38], the moving objects [39], humans [40, 41] and heavy equipment [42]. There have been many algorithms proposed for the purpose of optimizing path planning. Examples include Extended RRT (ERRT) [43], Dynamic RRT (DRRT) [44], hybrid GA [45], Simulated Annealing (SA) [46] and the Path Re-planner (PRP) [31]. In order to precisely control the motions of tower cranes operating in complex environments, adaptive [47, 48] and observer-based [49] controls can be used to avoid load swing and other undesired load movements involved in crane control.

The lifting schedule, which involves accurate determinations of starting and destination locations, is also of critical importance in ensuring the efficiency of material transportation. Zavichi et al. [50] defined the problem as the Crane Service Sequence Problem (CSSP) and set the material supply and demand locations as cities in the classic Traveling Salesman Problem (TSP). The problem was formulated as an integer programming problem, and the lifting schedule of a single crane was optimized to reduce total movement time. The additional constraints, such as the deadline of material requests [51] and minimal waiting time of the service request [52], were also taken into account and solved using GA and improved harmony search, respectively. Releasing the fixed pairs of routes from supply to demand locations, Huang et al. [13] formulated the CSSP as an MILP model that was solved using standard branch-and-bound techniques for the global optimum solution. Nearest Neighbor First (NNF), one of the heuristic methods widely applied in the TSP [53] and the Vehicle Routing Problem (VRP) [54], has been shown to obtain acceptable solutions in CSSP [13, 50]. However, the applicability of this research is limited due to its focus on only a single tower crane, and its findings cannot be employed in coordinating the operations of multiple tower cranes.

Previous research into approaches to avoid crane collisions inside overlapping areas can be classified as falling within two broad categories of research: (i) the optimization of path planning; and (ii) the optimization of lifting schedules. Theoretically, following a fixed schedule and properly arranging the lifting paths of multiple cranes can be an effective way to prevent potential collisions in an overlapping area. Practically, however, the use of anti-collision systems can only suspend cranes movements or tune movement velocity to ensure safety [55, 56]. Based on a given site layout and material requests, the optimization of lifting schedules aims to prevent collisions in overlapping areas guaranteed by the non-crossing spatial constraints [57]. Hattab et al. [14] proposed a simulation model for properly distributing lifting requests to two tower cranes to achieve balanced crane utilization and rearranging task sequences to prevent collisions in the overlapping area. Previous studies [14, 23, 24, 50, 58] fixed the pairs of supply locations and demand locations, which may have had the effect of sacrificing continuity of tower crane operation [3]. Khodabandelu et al. [3] proposed an ABS simulation model for selecting an appropriate supply point for each task in a way that reduces total operation time while preventing collisions. Although this system predetermined the priority of each task to reduce the number of possible schedules, the nature of the simulation process still cannot guarantee entirely optimal results.

3. Problem statement and assumptions

Given a construction site layout and lifting requests, the linkages between the requests and the locations of tower cranes and supply points can be used to determine optimized crane movements and transportation efficiency. For each single tower crane, the optimized selection of a supply point for a request and the implementation of an effective lifting schedule can lead to a high ratio of crane utilization. For multiple, overlapping tower cranes, the schedule design must also consider the coordination of adjacent cranes movements in ways that avoid the potential for collision in overlapping areas. In the proposed MCCSP, the problem was formulated as an MILP optimization model. The model achieves collision-free scheduling by forbidding simultaneous crane movements inside overlapping areas. It also optimizes the schedules of crane movements at minimum time-weighted energy cost by automatically 1) distributing the material requests in overlapping areas to appropriate tower cranes; 2) selecting the appropriate supply location to serve each request; and 3) arranging the lifting sequences of tower cranes to complete the requests. The MILP model was solved using the commercial software Gurobi^{TM} [59].

The study provides various pieces of relevant engineering information. Specifically, the positions of all the supply and demand locations on-site are predetermined; information about material storage and requests are project-specific and given by contractors; the velocity of tower cranes is set based on specifications. Four assumptions were implemented in the proposed optimization model:

- Each crane movement selects the shortest path along the minor arc between two locations;
- Each tower crane can only transport one type of material in each lifting;
- Each tower crane initially stays at a demand location in a schedule before starting a material transportation task; and
- Each overlapping area is limited to a small area that can only accommodate supply or demand locations.

4. The formulations of the proposed optimization method

The following sections explain the variables and constraints in the model. The objective function is introduced in Section 4.1. Section 4.2 briefly describes the calculation of the hook movement time between any two points using Eqs. (4)-(9) [13, 60]. In Section 4.3, the constraint sets (10) to (36) are introduced to formulate and control the material transportation process.

4.1 Objective function

The objective function of the proposed model is to minimize the time-weighted energy cost to complete all the given requests [61]. In Eq. (1), the energy cost comprises two parts, $\overline{C}$ and $\overline{\overline{C}}$. $\overline{C}$ represents the energy cost of the empty-loaded lifting that all cranes with an empty hook consume when moving from demand locations to supply locations. Similarly, $\overline{\overline{C}}$ signifies the energy cost of the fully-loaded lifting that all cranes with a fully loaded hook consume when moving from supply locations to demand locations. Table 1 lists explanation of the symbols used in the objective function section.

$$Min\left(\overline{C}+\overline{\overline{C}}\right) \tag{1}$$

In Eq. (2), a binary variable $z_{s,j,i,k}$ =1 represents that a tower crane at a location *k* with an empty-loaded hook moves from a demand location *j* to a supply location *i* in a lifting sequence *s*. $T_{i,j}^{k}$ is the movement time between the two locations. The empty hook will be loaded with materials at supply location *i,* and $T_{Loading}$ is the material loading time. A parameter $\overline{\Omega}$ stands for the estimated unit energy cost of empty-loaded lifting movements in a minute.

$$\overline{C}=\sum_{s=1}^{S}\sum_{i=1}^{I}\sum_{j=1}^{J}\sum_{k=1}^{K}\left(T_{i,j}^{k}+T_{Loading}\right)\cdot\overline{\Omega}\cdot z_{s,j,i,k} \tag{2}$$

Similarly in Eq. (3), a binary variable $y_{s,i,j,k,m}$ =1 indicates that a tower crane at a location *k* with a fully-loaded hook moves from a supply location *i* to a demand location *j* with material type *m* in a sequence *s*. The fully-loaded hook is unloaded at the demand location *j,* and $T_{Unloading}$ is the material unloading time. Similarly, $\overline{\overline{\Omega}}$ indicates the estimated unit energy cost of fully-loaded lifting movements in a minute.

$$\overline{\overline{C}}=\sum_{s=1}^{S}\sum_{i=1}^{I}\sum_{j=1}^{J}\sum_{k=1}^{K}\sum_{m=1}^{M}\left(T_{i,j}^{k}+T_{Unloading}\right)\cdot\overline{\overline{\Omega}}\cdot y_{s,i,j,k,m} \tag{3}$$

Table 1.
Parameters and variables in the objective function section

Symbol	Type	Expression
$\overline{C}$	Continuous variable	The total energy cost from material demand locations to material supply locations;
$\overline{\overline{C}}$	Continuous variable	The total energy cost from material supply locations to material demand locations;
$y_{s,i,j,k,m}$	Binary variable	$y_{s,i,j,k,m}$ =1 indicates a tower crane at a location *k* transports material type *m* from a supply location *i* to a demand location *j* in a work sequence *s*;
$z_{s,j,i,k}$	Binary variable	$z_{s,j,i,k}$ =1 indicates a tower crane at a location *k* travels from a demand location *j* to a supply location *i* in a work sequence *s*;
$T_{i,j}^{k}$	Continuous parameter	The hook movement time of a tower crane at location *k* between a supply location *i* and a demand location *j*;
$T_{Loading}$	Continuous parameter	The time to load materials from a material supply location;
$T_{Unloading}$	Continuous parameter	The time to unload materials to a material demand location;
$\overline{\Omega}$	Continuous parameter	The estimated unit energy cost of empty-loaded lifting movement in a minute;

$\overline{\overline{\Omega}}$	Continuous parameter	The estimated unit energy cost of fully-loaded lifting movement in a minute.

4.2 Estimate tower crane movement time between two locations

In Fig. 1, the tower crane movement can be divided into a horizontal movement and a vertical hosting movement. Table 2 lists the explanations of the parameters used in the following Eqs. (4)-(9). In Eq. (4), the crane movement time $T_{i,j}^{k}$ is calculated by the combination of horizontal movement time $T_{h(i,j)}^{k}$ and vertical movement time $T_{v(i,j)}^{k}$. Considering the simultaneous hook movement in the horizontal and vertical directions, a continuous parameter β_k ranging from 0.0 to 1.0 is introduced to realize the controller's operation level. The user input parameter γ_k ranging from 1.0 to 10.0 indicates the level of difficulty in operating a crane at a location *k* due to the different site conditions. To consider the constructed building on site or the heavy materials which might possibly lead to a longer and more complex movement path, the coefficient $\mu_{i,j}^{k}$ ranging between 1.0 and 10.0 is introduced. It denotes the complexity of the movement route between a supply location *i* and a demand location *j* while a crane sets up at a location *k*.

$$T_{i,j}^{k} = \mu_{i,j}^{k} \cdot \left[\gamma_k \cdot \left(\max\left(T_{h(i,j)}^{k}, T_{v(i,j)}^{k}\right) + \beta_k \cdot \min\left(T_{h(i,j)}^{k}, T_{v(i,j)}^{k}\right)\right)\right] \tag{4}$$

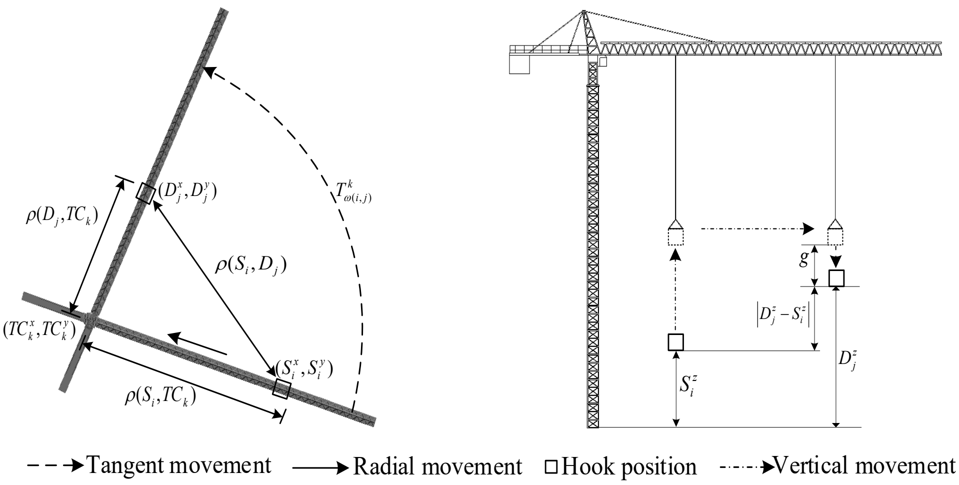

Fig. 1. An example of hook movement routes in horizontal direction (left) and in vertical direction (right)

Table 2.
Parameters in movement time estimation section

Symbol	Expression
S_i^x, S_i^y, S_i^z	Coordinates of a material supply location *i*;

D_j^x, D_j^y, D_j^z	Coordinates of a material demand location *j*;
TC_k^x, TC_k^y, TC_k^z	Coordinates of a tower crane setup at a location *k*;
$T_{h(i,j)}^k$	The horizontal hook movement time of a tower crane at location *k* between a supply location *i* and a demand location *j*;
$T_{v(i,j)}^k$	The hook movement time of a tower crane at location *k* between a supply location *i* and a demand location *j* in the vertical direction;
$T_{r(i,j)}^k$	The hook movement time along a jib of a tower crane at location *k* between a supply location *i* and a demand location *j*;
$T_{\omega(i,j)}^k$	The tangent hook movement time of a tower crane at location *k* between a supply location *i* and a demand location *j*;
V_r^k	The hook movement velocity along a jib of a tower crane at location *k*;
V_ω^k	The slewing velocity of a jib of a tower crane at location *k*;
V_h^k	The hoisting velocity of a hook of a tower crane at location *k*;
$\rho(S_i, TC_k)$	The distance between supply location *i* and a tower crane setup location *k*;
$\rho(D_j, TC_k)$	The distance between demand location *j* and a tower crane setup location *k*;
$\rho(S_i, D_j)$	The distance between a supply location *i* and a demand location *j*;
α_k	The degree of simultaneous hook movement in radial and tangential directions;
β_k	The degree of simultaneous hook movement in vertical and horizontal planes;
γ_k	The level of difficulty in operating a crane at a location *k*;
$\mu_{i,j}^k$	The complexity of the movement route between a supply location *i* and a demand location *j* while a crane sets up at a location *k*.

In Fig. 1.a, the horizontal movement can be split into the radial movement of a trolley and the slewing movement of a jib. Eq. (5) can calculate the simultaneous movement time by combining the movement time $T_{r(i,j)}^k$ and $T_{\omega(i,j)}^k$ in radial and tangent directions. A high value of a continuous parameter α_k ranging from 0 to 1 represents a low synchronous movement in the two directions.

$$T_{h(i,j)}^k = \max(T_{r(i,j)}^k, T_{\omega(i,j)}^k) + \alpha_k \cdot \min(T_{r(i,j)}^k, T_{\omega(i,j)}^k) \tag{5}$$

Eqs. (6)-(7) refer to the time taken for the radial movement and slewing movement between pairs of supply and demand locations. V_r^k and V_ω^k are the velocities in radial and tangent directions. $\rho(S_i, TC_k)$ is the Euclidean distance between a supply location *i* and a tower crane at a location *k,* which is calculated in Eq. (8). $\rho(D_j, TC_k)$ is the distance between a demand location and a tower crane location, and $\rho(S_i, D_j)$ represents the distance between a supply location and a demand location, which is calculated using similar equations.

$$T_{r(i,j)}^k = \frac{\left|\rho(S_i, TC_k) - \rho(D_j, TC_k)\right|}{V_r^k} \tag{6}$$

$$T_{\omega(i,j)}^{k} = \frac{1}{v_{\omega}^{k}} \times \arccos\left(\frac{\rho(S_i, TC_k)^2 + \rho(D_j, TC_k)^2 - \rho(S_i, D_j)^2}{2 \times \rho(S_i, TC_k) \times \rho(D_j, TC_k)}\right)$$

$$(0 \leq \arccos(\theta) \leq 180^{\circ}) \quad (7)$$

$$\rho(S_i, TC_k) = \sqrt{(S_i^x - TC_k^x)^2 + (S_i^y - TC_k^y)^2} \quad (8)$$

Illustrated in Fig. 1.b, the vertical movement distance from a supply location i to a demand location j includes the height difference represented by $\left|D_j^z - S_i^z\right|$ and the double minimum hoisting height g. The vertical movement time is calculated using Eq. (9), and V_h^k is the crane velocity in vertical direction.

$$T_{v(i,j)}^{k} = \frac{(\left|D_j^z - S_i^z\right| + 2 \cdot g)}{V_h^k} \quad (9)$$

4.3 Constraints of the proposed optimization model

To clarify the development of the proposed model, a general flowchart in Fig. 2 is given to illustrate the decision variables and constraints in the formulations. Based on a given site layout and the material requests, the optimization proceeds through the following six steps. It is recognized that these six steps cannot represent the exact flow basis of the proposed algorithm. Table 3 lists explanations of the parameters and variables in the constraint sets (10)-(21).

Table 3.
Parameters and variables in the constraints section

Symbol	Type	Expression
$\varepsilon_{r,j,m}$	Binary parameter	$\varepsilon_{r,j,m}$ =1 indicates a material request r from a demand location j needing material type m;
$\alpha'_{i,m}$	Binary parameter	$\alpha'_{i,m}$ =1 indicates material type m is available at material supply location i;
$\delta_{r,i,j,m}$	Binary variable	$\delta_{r,i,j,m}$ =1 indicates a supply location i is selected to provide material type m for a request r from a demand location j;
$x_{r,s,k}$	Binary variable	$x_{r,s,k}$ =1 indicates a tower crane at a location k completes a material request r in a work sequence s;
π_k	Continuous parameter	The crane coverage radius;
$\chi_{s,j,k}$	Binary variable	$\chi_{s,j,k}$ =1 indicates a tower crane at a location k must unload materials at the demand location j in the sequence s;
$\tau_{j,k}$	Binary Parameter	$\tau_{j,k}$ =1 indicates a tower crane at location k initially stays at a demand location j.

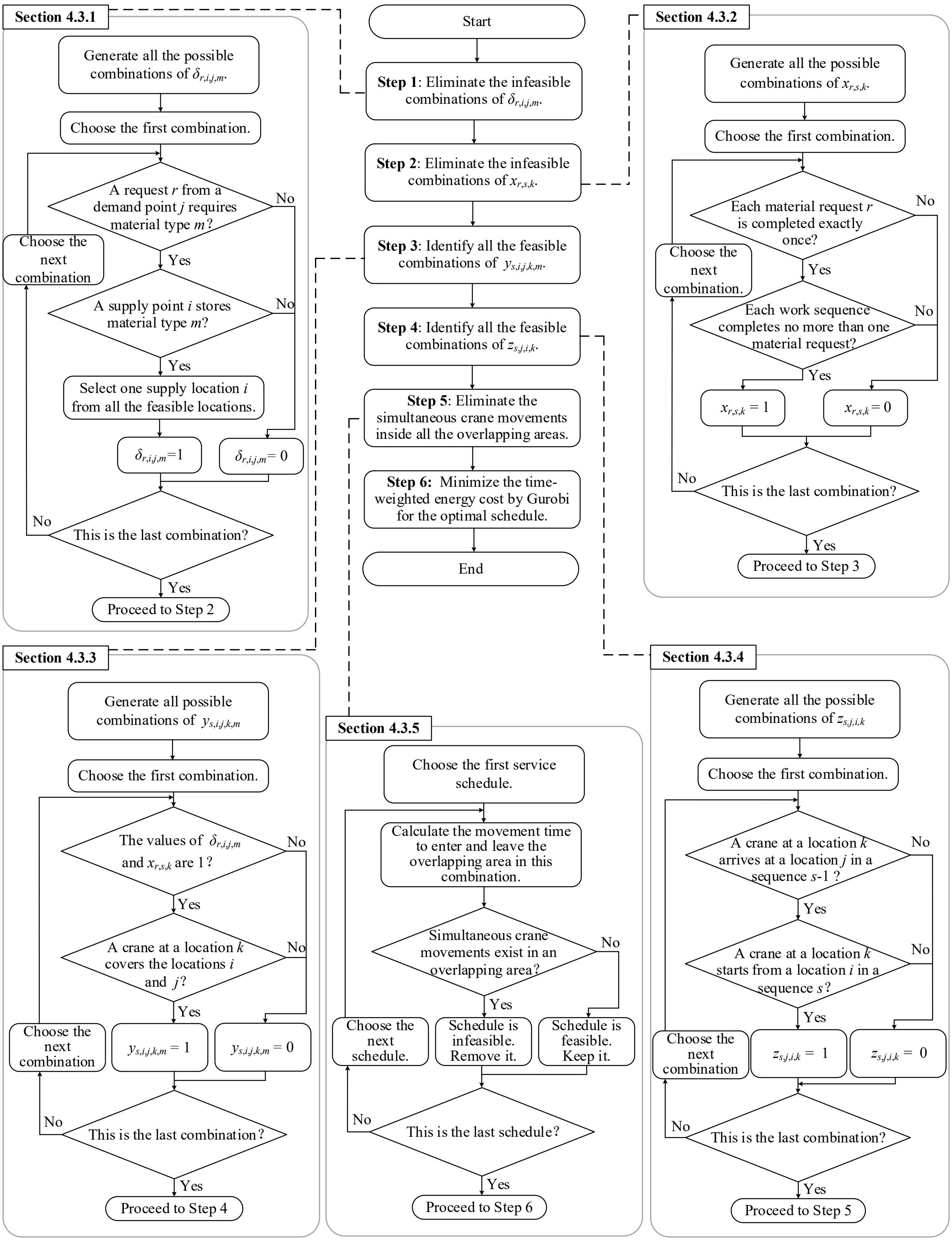

Fig. 2 General flowchart of proposed model

240

4.3.1 Eliminate infeasible linkages between supply and demand locations

In step 1, a binary variable $\delta_{r,i,j,m}$ is firstly introduced to link the pairs of supply and demand locations. In constraint set (10), if $\varepsilon_{r,j,m}$=1 and a material request *r* from a demand location *j* needs material type *m*, then $\sum_{i=1}^{I}\delta_{r,i,j,m}=1$ indicates that one supply location storing the material *m* must be assigned to support the request *r* from demand location *j*. Otherwise, $\varepsilon_{r,j,m}$ =0 and $\delta_{r,i,j,m}$ is forced to be 0. The constraint set (11) is set to identify whether a supply location *i* stores a material *m,* and this is determined by the given binary parameter $\alpha'_{i,m}$.

$$\sum_{i=1}^{I}\delta_{r,i,j,m}=\varepsilon_{r,j,m} \qquad \forall r \in \{1,2....,R\},$$

$$\forall j \in \{1,2....,J\}\ \forall m \in \{1,2....,M\} \quad (10)$$

$$\alpha'_{i,m} \geq \delta_{r,i,j,m} \qquad \forall r \in \{1,2....,R\}\ \forall i \in \{1,2....,I\}$$

$$\forall j \in \{1,2....,J\}\ \forall m \in \{1,2....,M\} \quad (11)$$

4.3.2 Eliminate infeasible combinations of request-assignments to tower cranes

In step 2, the binary variable $x_{r,s,k}$ represents the linkage of the request *r* and the lifting sequence *s* of a tower crane at location *k*. In constraint set (12), $\sum_{s=1}^{S}\sum_{k=1}^{K}x_{r,s,k}=1$ indicates that each material request *r* must be assigned to only one optimized lifting sequence of one tower crane. For each tower crane, each lifting sequence *s* can only select one material request at most in constraint set (13).

$$\sum_{s=1}^{S}\sum_{k=1}^{K}x_{r,s,k}=1 \qquad \forall r \in \{1,2....,R\} \quad (12)$$

$$\sum_{r=1}^{R}x_{r,s,k} \leq 1 \qquad \forall s \in \{1,2....,S\},\ \ \forall k \in \{1,2....,K\} \quad (13)$$

4.3.3 Generate feasible combinations of fully-loaded lifting movement

In step 3, the binary decision variable $y_{s,i,j,k,m}$ is used to mathematically identify fully-loaded crane movements from supply locations to demand locations. In constraint set (14), if both of the binary variables $x_{r,s,k}$ and $\delta_{r,i,j,m}$ are 1, it indicates that a material request *r* is assigned to a working sequence *s* of a tower crane at a location *k,* and the crane moves from a supply location i to a demand location j carrying material m. Then, $y_{s,i,j,k,m}$ must be 1 to confirm that the fully-loaded crane movement is conducted.

$$2 - x_{r,s,k} - \delta_{r,i,j,m} \geq 1 - y_{s,i,j,k,m}, \forall r \in \{1,2....,R\}, \forall s \in \{1,2....,S\}$$
$$\forall i \in \{1,2....,I\}, \forall j \in \{1,2....,J\}, \forall m \in \{1,2....,M\}, \forall k \in \{1,2....,K\} \quad (14)$$

Constraint sets (15) and (16) are introduced to ensure that the supply and demand locations in each fully-loaded movement are covered by the same tower crane. If either of $\rho(D_j, TC_k)$ or $\rho(S_i, TC_k)$ is larger than the crane coverage radius π_k, and the supply location or the demand location is out of the crane coverage, then, $y_{s,i,j,k,m}$ must be 0 and the fully-loaded movement cannot be completed. Constraint set (17) forces each fully-loaded movement in a sequence s only from one supply location with one type of material to a demand location.

$$y_{s,i,j,k,m} \cdot \left(\rho\left(D_j, TC_k\right) - \pi_k\right) \leq 0, \quad \forall s \in \{1,2....,S\}, \forall i \in \{1,2....,I\}$$
$$\forall j \in \{1,2....,J\}, \forall k \in \{1,2....,K\}, \forall m \in \{1,2....,M\} \quad (15)$$

$$y_{s,i,j,k,m} \cdot \left(\rho\left(S_i, TC_k\right) - \pi_k\right) \leq 0, \quad \forall s \in \{1,2....,S\}, \forall i \in \{1,2....,I\}$$
$$\forall j \in \{1,2....,J\}, \forall k \in \{1,2....,K\}, \forall m \in \{1,2....,M\} \quad (16)$$

$$\sum_{i=1}^{I} \sum_{j=1}^{J} \sum_{m=1}^{M} y_{s,i,j,k,m} = 1 \quad \forall s \in \{1,2....,S\}, \forall k \in \{1,2....,K\} \quad (17)$$

4.3.4 Generate feasible combinations of empty-loaded lifting movements

Step 4 aims to select the feasible empty-loaded lifting movements that are determined by the constraint sets (18) – (21). If $\varepsilon_{r,j,m}$=1 and $x_{r,s,k}$=1, which indicates that a request r from a demand location j requires material type m, and the request r is completed by a tower crane at a location k in a lifting sequence s, then the fully-loaded tower crane at a location k must unload materials at the demand location j in the sequence s and $\chi_{s,j,k}$=1.

$$2 - \varepsilon_{r,j,m} - x_{r,s,k} \geq 1 - \chi_{s,j,k}, \quad \forall r \in \{1,2....,R\}, \forall s \in \{1,2....,S\}$$
$$\forall m \in \{1,2....,M\}, \forall k \in \{1,2....,K\}, \forall j \in \{1,2....,J\} \quad (18)$$

In constraint set (19), for two consecutive lifting sequences s and s+1, if $\chi_{s,j,k}$=1 and $y_{s+1,i,o,k,m}$=1, which indicates that a fully-loaded crane movement stops at a demand location j in the sequence s and the next fully-loaded crane movement in the sequence s+1 starts from a supply location i, then $z_{s+1,j,i,k}$=1, which determines that the empty-loaded movement in the sequence s+1 must travel from the demand location j to the supply location i.

$$2-\chi_{s,j,k}-y_{s+1,i,o,k,m}\geq 1-z_{s+1,j,i,k}\,,\quad \forall s\in\{1,2....,S-1\},\forall i\in\{1,2....,I\}$$
$$\forall j,o\in\{1,2....,J\},\forall k\in\{1,2....,K\},\forall m\in\{1,2....,M\}\quad(19)$$

In the first sequence s=1, the empty-loaded lifting movement depends on the user-specified initial location and the following fully-loaded movement. In constraint set (20), a binary parameter $\tau_{j,k}$=1 signifies that the demand location j is the user-specified initial location where the first empty-loaded lifting movement starts. If $y_{s=1,i,o,k,m}$=1 and the following fully-loaded lifting movement begins from a supply location i, then $z_{s=1,j,i,k}$=1 and the first hook movement in the first working sequence travels from the user-specified demand location j to the supply location i. The constraint set (21) forces there to be only one empty-loaded movement that exists from a location j to a location i in each sequence s.

$$2-\tau_{j,k}-y_{s,i,o,k,m}\geq 1-z_{s,j,i,k}\qquad s=1\,,\forall i\in\{1,2....,I\}$$
$$\forall j,o\in\{1,2....,J\},\forall k\in\{1,2....,K\},\forall m\in\{1,2....,M\}(20)$$

$$\sum_{i=1}^{I}\sum_{j=1}^{J}z_{s,j,i,k}=1\qquad \forall s\in\{1,2....,S\},\forall k\in\{1,2....,K\}\quad(21)$$

4.3.5 Eliminate the service schedules of simultaneous movements inside overlapping areas

Based on the possible crane movements identified in the previous section, the following Eqs. (22)-(28) can identify the intersection point that a crane passes in a movement to enter or leave an overlapping area. The time to reach the point is estimated by Eqs. (29)-(33). The constraint sets (34)-(36) are introduced to eliminate any service schedules with simultaneous crane movements inside overlapping areas.

(1) Identify the movement routes passing overlapping areas

Given the positions of supply and demand locations, Figure 3 illustrates three typical scenarios of crane movements. Several parameters are introduced to illustrate the movements and explained in Table 4. Firstly, two binary parameters $\eta_{i,c}$ and $\lambda_{j,c}$ are used to denote whether the given locations are inside an overlapping area c. In Scenario 1, the demand location j is inside and a supply location i is outside. Then $\lambda_{j,c}$ is set to be 1 and $\eta_{i,c}$ is 0. In Eq. (22), $\overline{TP}^{k}_{h(i,p)}$ and $\overline{\overline{TP}}^{k}_{h(j,p)}$ represent the movement time from the intersection point p to each supply and demand location. The binary parameter $\overline{\theta}_{i,j,k,c,p}$ is used to identify whether a movement passes through an intersection point p. When the crane enters the overlapping area from the intersection point p and stays inside, the sum of $\overline{TP}^{k}_{h(i,p)}$ and $\overline{\overline{TP}}^{k}_{h(j,p)}$ is smaller than or equals $T^{k}_{h(i,j)}$ and this forces $\bar{\theta}_{i,j,k,c,p}$ to be 1. For the reverse movement starting from the demand location j, in Eq. (23), $\bar{\bar{\theta}}_{j,i,k,c,p}$ is set to equal $\bar{\theta}_{i,j,k,c,p}$, which means the reverse movement must pass the same intersection point p to leave the area.

$$\bar{\theta}_{i,j,k,c,p} = \begin{cases} 1, & \overline{TP}^{k}_{h(i,p)} + \overline{\overline{TP}}^{k}_{h(j,p)} \le T^{k}_{h(i,j)} \\ 0, & \overline{TP}^{k}_{h(i,p)} + \overline{\overline{TP}}^{k}_{h(j,p)} > T^{k}_{h(i,j)} \end{cases} \qquad \forall c \in \{1,2....,C\}$$

$$\forall p \in \{2c-1, 2c\}, \forall i \in \{1,2....,I\}, \forall j \in \{1,2....,J\}, \forall k \in \{1,2....,K\} \quad (22)$$

$$\bar{\bar{\theta}}_{j,i,k,c,p} = \bar{\theta}_{i,j,k,c,p} \qquad \forall c \in \{1,2....,C\},$$

$$\forall p \in \{2c-1, 2c\}, \forall i \in \{1,2....,I\}, \forall j \in \{1,2....,J\}, \forall k \in \{1,2....,K\} \quad (23)$$

Table 4.
Parameters used to identify the movement routes passing overlapping areas

Symbol	Type	Expression
$\eta_{i,c}$	Binary parameter	$\eta_{i,c}$ =1 indicates a supply location i exists in an overlapping area c;
$\lambda_{j,c}$	Binary parameter	$\lambda_{j,c}$ =1 indicates a demand location j exists in an overlapping area c;
$\overline{TP}^{k}_{h(i,p)}$	Continuous parameter	The movement time of a tower crane at location k between a supply location i to an intersection point p;
$\overline{\overline{TP}}^{k}_{h(j,p)}$	Continuous parameter	The movement time of a tower crane at location k between a demand location j to an intersection point p;
$TP^{k}_{h(c)}$	Continuous parameter	The movement time of a tower crane at location k passes through the overlapping area c;
$\bar{\theta}_{i,j,k,c,p}$	Binary parameter	$\bar{\theta}_{i,j,k,c,p}$ =1 indicates a tower crane at a location k moves from a supply location i to a demand location j by entering or leaving an overlapping area c through an intersection point p;
$\bar{\bar{\theta}}_{j,i,k,c,p}$	Binary parameter	$\bar{\bar{\theta}}_{j,i,k,c,p}$ =1 indicates a tower crane at a location k travels from a demand location j to a supply location i by entering or leaving an overlapping area c through an intersection point p;
$\theta_{i,j,k,c}$	Binary parameter	$\theta_{i,j,k,c}$ =1 indicates a movement of a tower crane at a location k between a supply location i and a demand location j passes through an overlapping area c.

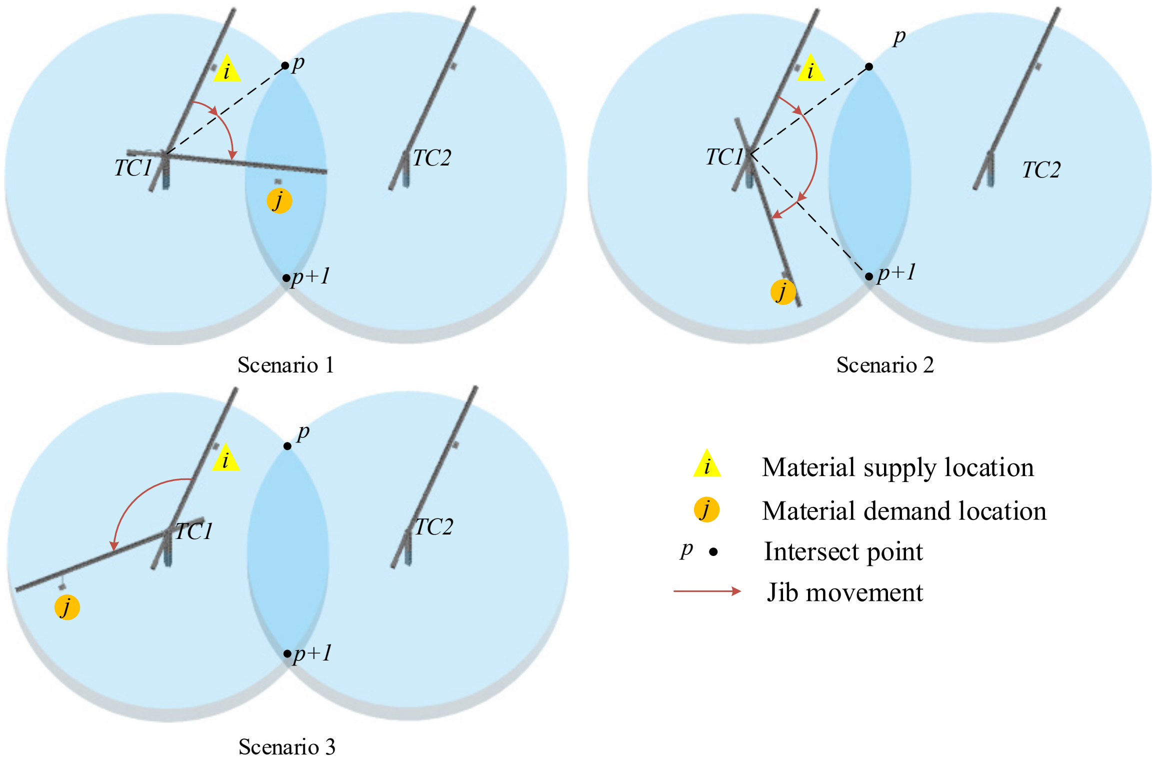

Fig. 3 The selection of an intersection point for the movement path starting from a supply location

In Scenarios 2 and 3, when the supply location and the demand location are out of the overlapping area, the parameters $\eta_{i,c}$ and $\lambda_{j,c}$ must be 0. In Scenario 2, the crane travels through the entire overlapping area. In Eqs. (24)-(25), $\overline{\theta}_{i,j,k,c,p}$ and $\overline{\theta}_{i,j,k,c,p+1}$ are used to identify the intersection point at which the crane enters the area. For the reverse movement starting from the demand location j, the crane must follow the reverse route and enter the area from the other intersection point. The values of the binary parameters $\overline{\overline{\theta}}_{j,i,k,c,p}$ and $\overline{\overline{\theta}}_{j,i,k,c,p+1}$ are controlled by Eqs. (26)-(27).

$$\overline{\theta}_{i,j,k,c,p}=\begin{cases}1, & \overline{TP}^{k}_{h(i,p)}+TP^{k}_{h(c)}+\overline{\overline{TP}}^{k}_{h(j,p+1)}\leq T^{k}_{h(i,j)}\\ 0, & \overline{TP}^{k}_{h(i,p)}+TP^{k}_{h(c)}+\overline{\overline{TP}}^{k}_{h(j,p+1)}> T^{k}_{h(i,j)}\end{cases} \qquad \forall c\in\{1,2....,C\},$$

$$p=2c-1,\forall i\in\{1,2....,I\},\forall j\in\{1,2....,J\} \tag{24}$$

$$\overline{\theta}_{i,j,k,c,p+1}=\begin{cases}1, & \overline{TP}^{k}_{h(i,p+1)}+TP^{k}_{h(c)}+\overline{\overline{TP}}^{k}_{h(j,p)}\leq T^{k}_{h(i,j)}\\ 0, & \overline{TP}^{k}_{h(i,p+1)}+TP^{k}_{h(c)}+\overline{\overline{TP}}^{k}_{h(j,p)}> T^{k}_{h(i,j)}\end{cases} \qquad \forall c\in\{1,2....,C\},$$

$$p=2c-1,\forall i\in\{1,2....,I\},\forall j\in\{1,2....,J\} \tag{25}$$

$$\overline{\overline{\theta}}_{j,i,k,c,p+1}=\overline{\theta}_{i,j,k,c,p} \qquad \forall c\in\{1,2....,C\},$$

$$p = 2c-1, \forall i \in \{1,2....,I\}, \forall j \in \{1,2....,J\} \quad (26)$$

$$\overline{\overline{\theta}}_{j,i,k,c,p} = \overline{\theta}_{i,j,k,c,p+1} \quad \forall c \in \{1,2....,C\},$$
$$p = 2c-1, \forall i \in \{1,2....,I\}, \forall j \in \{1,2....,J\} \quad (27)$$

In Scenario 3, the crane moves along the minor arc between the two locations without passing the overlapping area. Then, $\overline{\theta}_{i,j,k,c,p}$ and $\overline{\theta}_{i,j,k,c,p+1}$ in Eqs. (24) and (25) must be 0. The binary parameter $\theta_{i,j,k,c}$ indicating whether a movement passes an overlapping area is also forced to be 0 in Eq. (28). Table 5 summarizes the values of the binary parameters to mathematically illustrate the movements in the three scenarios.

$$\theta_{i,j,k,c} = \begin{cases} 1, & \overline{\theta}_{i,j,k,c,p} = 1 \quad or \quad \overline{\theta}_{i,j,k,c,p+1} = 1 \\ 0, & \overline{\theta}_{i,j,k,c,p} = 0 \quad and \quad \overline{\theta}_{i,j,k,c,p+1} = 0 \end{cases} \quad \forall c \in \{1,2....,C\},$$
$$p = 2c-1, \forall i \in \{1,2....,I\}, \forall j \in \{1,2....,J\} \quad (28)$$

Table 5.
The value of the binary parameters to identify the movements routes in the three scenarios

Scenario	The binary parameters							Equations
	$\eta_{i,c}$	$\lambda_{j,c}$	$\overline{\theta}_{i,j,k,c,p}$	$\overline{\theta}_{i,j,k,c,p+1}$	$\overline{\overline{\theta}}_{j,i,k,c,p}$	$\overline{\overline{\theta}}_{j,i,k,c,p+1}$	$\theta_{i,j,k,c}$	
1	0	1	1	0	1	0	1	22-23, 28
2	0	0	1	0	0	1	1	24-28
3	0	0	0	0	0	0	0	24-28

(2) **Estimate the time of each movement to enter and leave an overlapping area**

Several parameters and variables are introduced in this section and explained in Table 6. In Eqs. (29-a)-(29-c), a continuous variable $ST_{k,s,q}$ is firstly introduced to represent the starting time of each movement. In Eq. (29-a), for the empty-loaded lifting movement (q=1) in the first sequence (s=1), the starting time is set to be a given parameter BT_k. For each fully-loaded lifting movement (q=2), $ST_{k,s,q}$ in Eq. (29-b) equals the sum of the starting time of the empty-loaded lifting movement (q=1) in the sequence s and the movement time $T_{i,j}^{k}$. For the empty-loaded lifting movement (q=1) in the rest sequences (s≥2), $ST_{k,s,q}$ in Eq. (29-c) equals the sum of the starting time of the fully-loaded lifting movement (q=2) in the previous sequence (s-1) and the movement time $T_{i,j}^{k}$. For each movement, the supply location i and demand location j are identified by $y_{s,i,j,k,m}$ or $z_{s,j,i,k}$. $T_{Loading}$ and $T_{Unloading}$ indicate the extra material loading and unloading time.

$$ST_{k,s,q} = BT_k \qquad q=1, s=1, \forall k \in \{1,...K\} \quad (29\text{-a})$$

$$ST_{k,s,q} = ST_{k,s,q-1} + \sum_{i=1}^{I}\sum_{j=1}^{J} z_{s,j,i,k} \cdot \left(T_{i,j}^{k} + T_{Loading}\right)$$

$$q=2, \forall s \in \{1,...S\}, \forall k \in \{1,...K\} \quad (29\text{-b})$$

$$ST_{k,s,q} = ST_{k,s-1,q+1} + \sum_{i=1}^{I}\sum_{j=1}^{J}\sum_{m=1}^{M} y_{s-1,i,j,k,m} \cdot \left(T_{i,j}^{k} + T_{Unloading}\right)$$

$$q=1, \forall s \in \{2,...S\}, \forall k \in \{1,...K\} \quad (29\text{-c})$$

Table 6.
Parameters in estimating the time of each movement to enter and leave an overlapping area

Symbol	Type	Expression
BT_k	Continuous parameter	The starting time of each tower crane;
$ST_{k,s,q}$	Continuous variable	The starting time of each movement;
$TI_{k,s,q,c}$	Continuous variable	The time of a tower crane set up at location k entering an overlapping area c in a movement q of a work sequence s;
$\overline{TI}_{s,i,j,k,q,c}$	Continuous variable	The time from a supply location i or a demand location j to the selected intersection point of overlapping area c;
$TO_{k,s,q,c}$	Continuous variable	The time of a tower crane set up at location k leaving an overlapping area c in a movement q of a work sequence s;
$\overline{TO}_{s,i,j,k,q,c}$	Continuous variable	The movement time from entering the overlapping area to leaving the area.

In Eq. (30), the variable $TI_{k,s,q,c}$ is defined as the time for a crane to enter an overlapping area by reaching an intersection point. It is calculated by adding $ST_{k,s,q}$ with $\sum_{i=1}^{I}\sum_{j=1}^{J}\overline{TI}_{s,i,j,k,q,c}$, which is the time from a supply location i or a demand location j to the selected intersection point of overlapping area c.

$$TI_{k,s,q,c} = ST_{k,s,q} + \sum_{i=1}^{I}\sum_{j=1}^{J}\overline{TI}_{s,i,j,k,q,c}$$

$$\forall k \in \{1,2....,K\}, \forall s \in \{1,2....,S\}, \forall q \in \{1,2\}, \forall c \in \{1,2....,C\} \quad (30)$$

In Eqs. (31-a)-(31-g), the variable $\overline{TI}_{s,i,j,k,q,c}$ is calculated based on the classification of the crane movements. For the empty-loaded lifting movement (q=1) in the first sequence (s=1), when $\lambda_{j,c}$=1 and the movement starts from a demand location j inside an overlapping area c, the time to enter the area is set to be 0 in Eq. (31-a). In Eqs. (31-b) and (31-c), if a movement starts from a location inside the overlapping area c ($\lambda_{j,c}$=1 or $\eta_{i,c}$=1), then the crane must have already moved into the area in the last movement. $\overline{TI}_{s,i,j,k,q,c}$ is set to be a negative arbitrary large number M. For the lifting movement (q=1 or q=2) starting from a demand location or a supply location out of the overlapping area c ($\lambda_{j,c}$=0 or $\eta_{i,c}$=0), the parameter $\theta_{i,j,k,c}$ must be 1 if the crane enters the area. Then, in Eqs. (31-d) and (31-e), $\overline{TI}_{s,i,j,k,q,c}$ equals the time from the starting location to the selected intersection point identified by the pair of $\overline{\theta}_{i,j,k,c,p}$ and $\overline{\theta}_{i,j,k,c,p+1}$ or the pair of $\overline{\overline{\theta}}_{i,j,k,c,p}$ and $\overline{\overline{\theta}}_{j,i,k,c,p+1}$. If a movement follows a route without passing through any overlapping area ($\lambda_{j,c}$=0 and $\eta_{i,c}$=0 and $\theta_{i,j,k,c}$=0), $\overline{TI}_{s,i,j,k,q,c}$ is set to be a negative arbitrary large number M in Eqs. (31-f) and (31-g).

$$\overline{TI}_{s,i,j,k,c} = 0 \qquad \theta_{i,j,k,c} = 1, s = 1, q = 1, \lambda_{j,c} = 1, \eta_{i,c} = 0$$
$$\forall i \in \{1,2....I\}, \forall j \in \{1,2....J\}, \forall c \in \{1,2....C\}, \forall k \in \{1,2....K\} \text{(31-a)}$$

$$\overline{TI}_{s,i,j,k,c} = -M \cdot \sum_{m=1}^{M} y_{s,i,j,k,m}$$
$$\theta_{i,j,k,c} = 1, \forall s \in \{2,...S\}, q = 1, \lambda_{j,c} = 1, \eta_{i,c} = 0$$
$$\forall i \in \{1,2....I\}, \forall j \in \{1,2....J\}, \forall c \in \{1,2....C\}, \forall k \in \{1,2....K\} \text{(31-b)}$$

$$\overline{TI}_{s,i,j,k,c} = -M \cdot z_{s,j,i,k}$$
$$\theta_{i,j,k,c} = 1, \forall s \in \{1,...S\}, q = 2, \lambda_{j,c} = 0, \eta_{i,c} = 1$$
$$\forall i \in \{1,2....I\}, \forall j \in \{1,2....J\}, \forall c \in \{1,2....C\}, \forall k \in \{1,2....K\} \text{(31-c)}$$

$$\overline{TI}_{s,i,j,k,c} = z_{s,j,i,k} \cdot \left[(\overline{\overline{\theta}}_{j,i,k,c,p} \cdot \overline{\overline{TP}}^{k}_{h(j,p)}) + (\overline{\overline{\theta}}_{j,i,k,c,p+1} \cdot \overline{\overline{TP}}^{k}_{h(j,p+1)}) \right]$$
$$\theta_{i,j,k,c} = 1, \forall s \in \{1,...S\}, q = 1, \lambda_{j,c} = 0, \forall \eta_{i,c} \in \{0,1\}$$
$$\forall i \in \{1,2....I\}, \forall j \in \{1,2....J\}, \forall c \in \{1,2....C\}, \forall k \in \{1,2....K\} \text{(31-d)}$$

$$\overline{TI}_{s,i,j,k,c} = \sum_{m=1}^{M} y_{s,i,j,k,m} \cdot \left[(\overline{\theta}_{i,j,k,c,p} \cdot \overline{TP}^{k}_{h(i,p)}) + (\overline{\theta}_{i,j,k,c,p+1} \cdot \overline{TP}^{k}_{h(i,p+1)}) \right]$$
$$\theta_{i,j,k,c} = 1, \forall s \in \{1,...S\}, q = 2, \forall \lambda_{j,c} \in \{0,1\}, \eta_{i,c} = 0$$

$$\forall i \in \{1,2....I\}, \forall j \in \{1,2....J\}, \forall c \in \{1,2....C\}, \forall k \in \{1,2....K\} \quad \text{(31-e)}$$

$$\overline{TI}_{s,i,j,k,c} = -M \cdot \sum_{m=1}^{M} y_{s,i,j,k,m}$$
$$\theta_{i,j,k,c} = 0, \forall s \in \{1,...S\}, q = 2, \lambda_{j,c} = 0, \eta_{i,c} = 0$$
$$\forall i \in \{1,2....I\}, \forall j \in \{1,2....J\}, \forall c \in \{1,2....C\}, \forall k \in \{1,2....K\} \quad \text{(31-f)}$$

$$\overline{TI}_{s,i,j,k,c} = -M \cdot z_{s,j,i,k}$$
$$\theta_{i,j,k,c} = 0, \forall s \in \{1,...S\}, q = 1, \lambda_{j,c} = 0, \eta_{i,c} = 0$$
$$\forall i \in \{1,2....I\}, \forall j \in \{1,2....J\}, \forall c \in \{1,2....C\}, \forall k \in \{1,2....K\} \quad \text{(31-g)}$$

The time of a movement to leave an overlapping area is represented by $TO_{k,s,q,c}$ and calculated in Eq. (32). $\sum_{i=1}^{I}\sum_{j=1}^{J}\overline{TO}_{s,i,j,k,q,c}$ consists of the movement time from entering the area to leaving the area by reaching the intersection points.

$$TO_{k,s,q,c} = TI_{k,s,q,c} + \sum_{i=1}^{I}\sum_{j=1}^{J}\overline{TO}_{s,i,j,k,q,c} \qquad \forall k \in \{1,2....K\},$$
$$\forall s \in \{1,2....S\}, \forall q \in \{1,2\}, \forall c \in \{1,2....C\} \quad \text{(29)}$$

In Eq. (33-a), for the lifting movement (q=1) in the first sequence (s=1), when a crane moves out from a demand location j inside the area ($\lambda_{j,c}$=1), $\overline{TO}_{s,i,j,k,q,c}$ is the time from the location j to an intersection point identified by the pair of the parameters $\bar{\bar{\theta}}_{j,i,k,c,p}$ or $\bar{\bar{\theta}}_{j,i,k,c,p+1}$. For the lifting movement (q=2) in the last sequence (s=S) starting from the supply location in the outside ($\eta_{i,c}$=0), if the crane finally stays inside the area ($\lambda_{j,c}$=1 and $\theta_{i,j,k,c}$=1), then $\overline{TO}_{s,i,j,k,q,c}$ is set to be an arbitrary large number M in Eq. (33-b). For other pairs of two consecutive movements that must load or unload materials inside an overlapping area ($\lambda_{j,c}$=1 or $\eta_{i,c}$=1), in Eqs. (33-c) and (33-d), $\overline{TO}_{s,i,j,k,q,c}$ consists of the time for the previous movement from an intersection point to a location inside and the time for the following movement from the location to an intersection point to leave the area. Material loading $T_{Loading}$ and unloading time $T_{Unloading}$ are also considered in this scenario. When the crane directly passes the entire area c ($\theta_{i,j,k,c}$=1), $\overline{TO}_{s,i,j,k,q,c}$ equals $TP^{k}_{h(c)}$, which is the movement time between the two intersection points. In Eq. (33-f), for the lifting movement (q=1 or q=2) starting from the location outside the overlapping area ($\lambda_{j,c}$=0 or $\eta_{i,c}$=0) without passing any overlapping area

($\theta_{i,j,k,c}$=0), $\overline{TO}_{s,i,j,k,q,c}$ is set to be 0. A pseudo-code is attached in Appendix I to explain the process used to calculate the time for a crane to enter and leave an overlapping area.

$$\overline{TO}_{s,i,j,k,c} = z_{s,j,i,k} \cdot \left[\left(\overline{\overline{\theta}}_{j,i,k,c,p} \cdot \overline{\overline{TP}}^{k}_{h(j,p)} \right) + \left(\overline{\overline{\theta}}_{j,i,k,c,p+1} \cdot \overline{\overline{TP}}^{k}_{h(j,p+1)} \right) \right]$$
$$\theta_{i,j,k,c} = 1, s = 1, q = 1, \lambda_{j,c} = 1, \eta_{i,c} = 0$$
$$\forall i \in \{1,2....I\}, \forall j \in \{1,2....J\}, \forall c \in \{1,2....C\}, \forall k \in \{1,2....K\} \quad \text{(30-a)}$$

$$\overline{TO}_{s,i,j,k,c} = M \cdot \sum_{m=1}^{M} y_{s,i,j,k,m}$$
$$\theta_{i,j,k,c} = 1, s = S, q = 2, \lambda_{j,c} = 1, \eta_{i,c} = 0$$
$$\forall i \in \{1,2....I\}, \forall j \in \{1,2....J\}, \forall c \in \{1,2....C\}, \forall k \in \{1,2....K\} \quad \text{(31-b)}$$

$$\overline{TO}_{s,i,j,k,c} = z_{s,n,i,k} \cdot \left[(\overline{\overline{\theta}}_{j,n,k,c,p} \cdot \overline{TP}^{k}_{h(n,p)}) + (\overline{\overline{\theta}}_{j,n,k,c,p+1} \cdot \overline{TP}^{k}_{h(n,p+1)}) + T_{Loading} \right]$$
$$+ \sum_{m=1}^{M} y_{s,i,j,k,m} \cdot \left[(\overline{\theta}_{i,j,k,c,p} \cdot \overline{TP}^{k}_{h(i,p)}) + (\overline{\theta}_{i,j,k,c,p+1} \cdot \overline{TP}^{k}_{h(i,p+1)}) \right]$$
$$\theta_{i,j,k,c} = 1, \forall s \in \{1,...S\}, q = 1, \lambda_{j,c} = 0, \eta_{i,c} = 1$$
$$\forall i \in \{1,2....I\}, \forall j \in \{1,2....J\}, \forall c \in \{1,2....C\}, \forall k \in \{1,2....K\} \quad \text{(32-c)}$$

$$\overline{TO}_{s,i,j,k,c} = \sum_{m=1}^{M} y_{s,i,j,k,m} \cdot \left[(\overline{\theta}_{i,j,k,c,p} \cdot \overline{\overline{TP}}^{k}_{h(j,p)}) + (\overline{\theta}_{i,j,k,c,p+1} \cdot \overline{\overline{TP}}^{k}_{h(j,p+1)}) + T_{Unloading} \right]$$
$$+ z_{s+1,j,o,k} \cdot \left[(\overline{\overline{\theta}}_{j,o,k,c,p} \cdot \overline{\overline{TP}}^{k}_{h(j,p)}) + (\overline{\overline{\theta}}_{j,o,k,c,p+1} \cdot \overline{\overline{TP}}^{k}_{h(j,p+1)}) \right]$$
$$\theta_{i,j,k,c} = 1, \forall s \in \{1,...S-1\}, q = 2, \lambda_{j,c} = 1, \eta_{i,c} = 0$$
$$\forall i \in \{1,2....I\}, \forall j \in \{1,2....J\}, \forall c \in \{1,2....C\}, \forall k \in \{1,2....K\} \quad \text{(33-d)}$$

$$\overline{TO}_{s,i,j,k,c} = TP^{k}_{h(c)}$$
$$\theta_{i,j,k,c} = 1, \forall s \in \{1,...S\}, \forall q \in \{1,2\}, \lambda_{j,c} = 0, \eta_{i,c} = 0$$
$$\forall i \in \{1,2....I\}, \forall j \in \{1,2....J\}, \forall c \in \{1,2....C\}, \forall k \in \{1,2....K\} \quad \text{(34-e)}$$

$$\overline{TO}_{s,i,j,k,c} = 0$$
$$\theta_{i,j,k,c} = 0, \forall s \in \{1,...S\}, \forall q \in \{1,2\}, \lambda_{j,c} = 0, \eta_{i,c} = 0$$
$$\forall i \in \{1,2....I\}, \forall j \in \{1,2....J\}, \forall c \in \{1,2....C\}, \forall k \in \{1,2....K\}, \quad \text{(35-f)}$$

(3) Forbid simultaneous movements inside overlapping areas

Fig. 4 illustrates the possible movements of two tower cranes crossing over an overlapping area. In Scenario 1, the crane at the location k=1 moves from the supply location i=1 and firstly enters an overlapping area at the time TI_1 from the intersection point p. Before it moves out from the point p+1 at the time TO_1, the crane at the location k=2 moves into the area at the time

TI_2 from the intersection point p. A parameter TS is a user-input threshold time or area to provide additional security against simultaneous movements inside the area. A continuous variable $WT^{l,u,h}_{k,s,q,c}$ represents the time difference between the movements q and h of two cranes at locations k and l in the working sequences s and u to leave and enter the same overlapping area c. The time difference WT is calculated in Eq. (34). Specifically in Scenario 1, $WT_{2\text{-}1}$ equal the sum of TO_2, and TS minus TI_1. $WT_{1\text{-}2}$ is the sum of TO_1 with TS minus TI_2. It is noted that the two positive values of $WT_{2\text{-}1}$ and $WT_{1\text{-}2}$ denote the simultaneous crane movements in an overlapping area.

In Scenario 2, when the crane at the location k=3 leaves from the point p at the time TO_3, the crane at the location k=4 cannot enter the threshold area. This is to enhance safety. The opposite signs of the continuous variables $WT_{3\text{-}4}$ and $WT_{4\text{-}3}$ can ensure that an overlapping area is monopolized by one tower crane during its movement inside the area.

$$WT^{l,u,h}_{k,s,q,c} = TO_{l,u,h,c} + TS - TI_{k,s,q,c} \qquad \forall k,l \in \{1,\ldots.K\}, k \neq l,$$

$$\forall s,u \in \{1,2\ldots.S\}, \forall q,h \in \{1,2\}, \forall c \in \{1,2\ldots.C\} \quad (36)$$

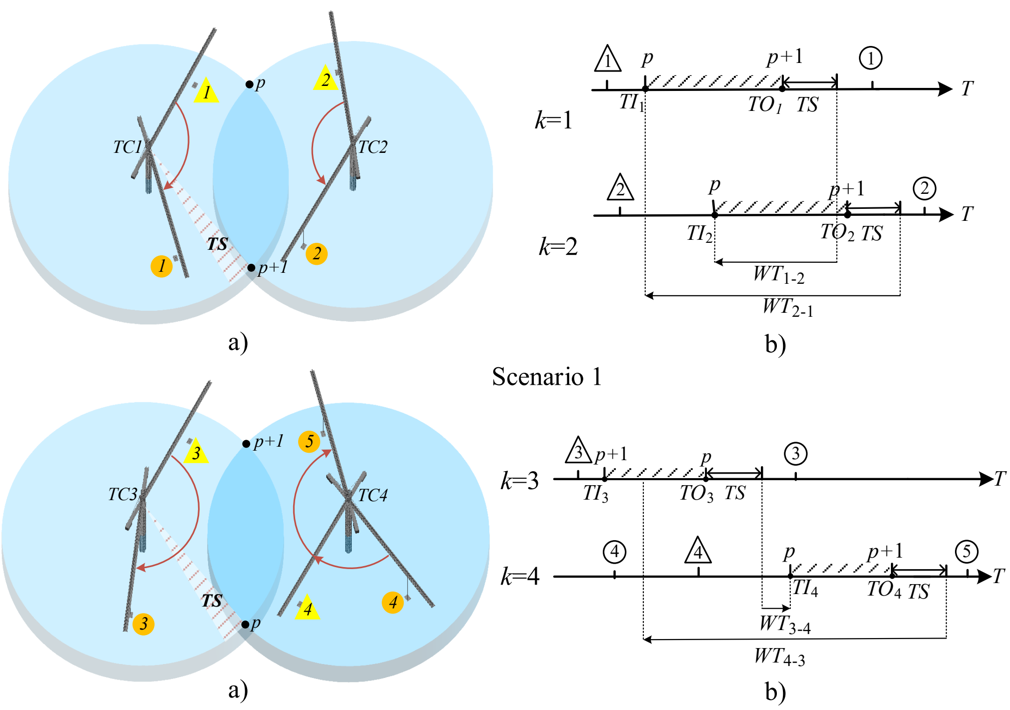

Scenario 2

△1 Material supply location 1 ① Material demand location p ● Intersection point p

TI_1, TO_1 The time to enter and leave an overlapping area TS The threshold time

Fig. 4 The possible movements of two adjacent tower cranes

The constraint sets (35)-(36) are introduced to guarantee the opposite signs of any pairs of

$WT_{k,s,q,c}^{l,u,h}$ and $WT_{l,u,h,c}^{k,s,q}$ to avoid simultaneous movements in any overlapping area. In constraint set (35), a positive value of $WT_{k,s,q,c}^{l,u,h}$ forces a binary variable $\psi_{k,s,q,c}^{l,u,h}$ to be 1, and a negative value of $WT_{k,s,q,c}^{l,u,h}$ forces $\psi_{k,s,q,c}^{l,u,h}$ to be 0. $\psi_{k,s,q,c}^{l,u,h}$=1 represents that the time difference between the two crane movements *q* and *h* of two cranes at locations *k* and *l* in the working sequences *s* and *u* to enter or leave an overlapping area *c* cannot be negative. The constraint set (36) is used to ensure that the values of the binary variables $\psi_{k,s,q,c}^{l,u,h}$ and $\psi_{k,s,q,c}^{l,u,h}$ must be either 1 or 0 and cannot be 1 simultaneously.

$$N \cdot \left(\psi_{k,s,q,c}^{l,u,h} - 1\right) \leq WT_{k,s,q,c}^{l,u,h} \leq N \cdot \psi_{k,s,q,c}^{l,u,h} \qquad \forall k,l \in \{1,....K\}, k \neq l,$$

$$\forall s,u \in \{1,2....S\}, \forall q,h \in \{1,2\}, \forall c \in \{1,2....C\} \quad (37)$$

$$1 - \psi_{l,u,h,c}^{k,s,q} - \psi_{k,s,q,c}^{l,u,h} \geq 0 \qquad \forall k,l \in \{1,....K\}, k \neq l,$$

$$\forall s,u \in \{1,2....S\}, \forall q,h \in \{1,2\}, \forall c \in \{1,2....C\} \quad (38)$$

The problem is formulated as an MILP model. The model is coded in Python 3.6 and solved using Gurobi™ [59] to find the global optimum solution.

5. Numerical example

The proposed optimization model was tested by a numerical example. As illustrated in Fig. 5, the construction project involves three 8-12 story buildings. To accelerate the construction process, four tower cranes were deployed on-site during the construction stage. Fourteen demand locations and seven supply locations were predetermined on site. Four demand locations and two supply locations were allocated inside the overlapping areas, including *D*2, *D*3, *D*4, *D*6, *S*3 and *S*4. Each supply location was able to store multiple types of material. Four types of material involved panel formwork, precast concrete facade units, and reinforcing bars and steels. Table 7 lists the coordinates of the supply locations and the different types of materials stored at each location. Table 8 gives the coordinates of the tower crane setup locations. Table 9 specifies the coordinates and the material request of each demand location.

Four tower cranes of 278 EC-B 12 Fibre Flat-Top were selected and deployed. Based on the technical specifications, radial velocity V_r^k=60 m/min, slewing velocity V_ω^k=0.5 rad/min, hoisting velocity V_h^k=136 m/min, and maximum radius π_k=70 m. The parameters of operator skills, α_k and β_k, were set to be 0 and 1.0. The coefficient γ_k and $\mu_{i,j}^{k}$ were set to be 1 based on the normal site conditions and low buildings. Material loading time $T_{Loading}$ and unloading time $T_{Unloading}$ were set to be 1.0 minute. Cost-weighted parameter $\overline{\Omega}$ and $\overline{\overline{\Omega}}$ were set to be 3.0 and 6.0 CNY/min [19, 22] respectively.

Table 7.

Details of material supply locations in the numerical example.

Material supply location, i	Location coordinates			Types of material supply, m
	x	y	z	
1	135	260	1.5	reinforcing bars (3), steels (4)
2	185	235	2	large panel formwork (1), precast concrete facade units (2)
3	52	146	1	large panel formwork (1), reinforcing bars (3), steels (4)
4	52	106	0	precast concrete facade units (2)
5	220	125	2	large panel formwork (1), steels (4)
6	220	75	1.5	precast concrete facade units (2), reinforcing bars (3)
7	0	170	0	large panel formwork (1), precast concrete facade units (2)

Table 8.

The coordinates of tower crane setup locations in the numerical example.

Crane setup location, k	Location coordinates		
	x	y	z
1	160	215	35
2	92	130	40
3	195	115	45
4	5	125	30

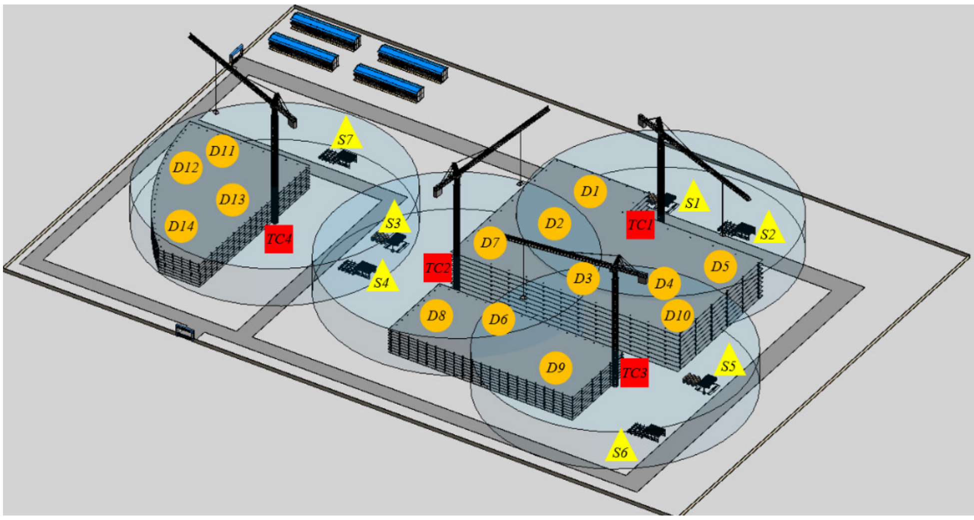

Fig. 5 The layout of the construction site

Table 9. Details of material demand locations and material requests in the numerical example.

Material demand location, *j*	Location coordinates *x*	*y*	*z*	Material request, *r*	Material type, *m*
1	110	222.5	20	12	2
2	120	180	20	11	4
				7	3
3	150	157.5	20	5	1
				6	2
4	187	170	20	10	4
5	210	195	20	4	3
6	142	116	20	15	1
7	80	180	20	8	4
8	115	85	20	1	2
9	158	75	20	9	3
10	220	157.5	20	16	4
11	-34	157	20	14	3
12	-48	139	20	3	4
13	-40	114	20	13	2
14	-30	95	20	2	1

In the numerical example, the passive coordination strategy and two optimization models for CSSP and MCSSP were used, and the solutions are presented for comparison and discussion. A daily lifting schedule of sixteen material requests was given for the passive coordination strategy. The crane signal man prioritized the requests and distributed them to each tower crane.

The lifting sequence of each tower crane is listed in Table 10. Columns 4 and 5 specify the starting locations and destinations of each movement. To avoid potential conflicts, the cranes at locations k=1 and k=2 are required to stop and wait for five times during the movements. The movements are detailed in Fig. 6. The movement cost and the cumulative cost are listed in columns 8 and 9. Employing the passive coordination strategy, the four tower cranes required 186.89 min (49.36+57.05+39.21+41.27) and 817.71 CNY to complete all the material requests.

Table 10. Details of crane movements arranged by the passive coordination strategy

Crane location, k	Lifting sequence, s	Material request, r	Hook movement		Movement cost, min	Waiting time, min	Movement cost, CNY*	Cumulative cost, CNY
			Start	End				
1	1	4	*D*5	*S*1	5.10	-	18.30	18.30
			*S*1	*D*5	5.10	-	36.60	54.90
	2	7	*D*5	*S*1	5.10	-	18.30	73.20
			*S*1	*D*3	5.11	-	36.66	109.86
	3	11	*D*3	*S*1	5.11	0.89(0.74+0.25)	21.00	130.86
			*S*1	*D*2	3.75	-	28.50	159.36
	4	12	*D*2	*S*2	6.38	-	22.14	181.50
			*S*2	*D*1	4.82	-	34.92	216.42
2	1	1	*D*2	*S*4	5.44	-	19.32	19.32
			*S*4	*D*8	3.17	-	25.02	44.34
	2	5	*D*8	*S*3	5.00	3.50(3.25+0.25)	28.50	72.84
			*S*3	*D*3	4.83	4.56(4.31+0.25)	62.34	135.18
	3	6	*D*3	*S*4	6.29	3.04(2.79+0.25)	30.99	166.17
			*S*4	*D*3	6.29	-	43.74	209.91
	4	8	*D*3	*S*3	4.83	-	17.49	227.40
			*S*3	*D*7	2.10	-	18.60	246.00
3	1	9	*D*6	*S*6	4.45	-	16.35	16.35
			*S*6	*D*9	2.76	-	22.56	38.91
	2	10	*D*9	*S*5	5.54	-	19.62	58.53
			*S*5	*D*4	2.85	-	23.10	81.63
	3	15	*D*4	*S*5	2.85	-	11.55	93.18
			*S*5	*D*6	5.63	-	39.78	132.96
	4	16	*D*6	*S*5	5.63	-	19.89	152.85
			*S*5	*D*10	1.50	-	15.00	167.85
4	1	2	*D*11	*S*7	1.67	-	8.01	8.01
			*S*7	*D*14	4.46	-	32.76	40.77
	2	3	*D*14	*S*3	5.82	-	20.46	61.23
			*S*3	*D*12	5.04	-	36.24	97.47
	3	13	*D*12	*S*7	2.53	-	10.59	108.06
			*S*7	*D*13	3.52	-	27.12	135.18
	4	14	*D*13	*S*3	6.04	-	21.12	156.30
			*S*3	*D*11	4.19	-	31.14	187.44

*: Movement cost includes operation cost, loading or unloading operation cost and waiting cost.

Fig. 6 depicts the crane movements as arranged by the passive coordination strategy. Each line represents a crane movement, while the green lines represent crane waiting time. For example, the tower crane at location k=4 moved into the overlapping area c=4 at 11.32 min. Before it left the area at 16.03 min, the tower crane at location k=2 planned to enter the same area at 12.78 min. To avoid a possible collision, it was arranged for the tower crane at location k=2 to wait outside until after the other crane left. The waiting time was 3.25 min (16.03-12.78) with an additional 0.25 min for the threshold distance. Then, the tower crane must enter the area c=4 no earlier than 16.28 min (16.03+0.25).

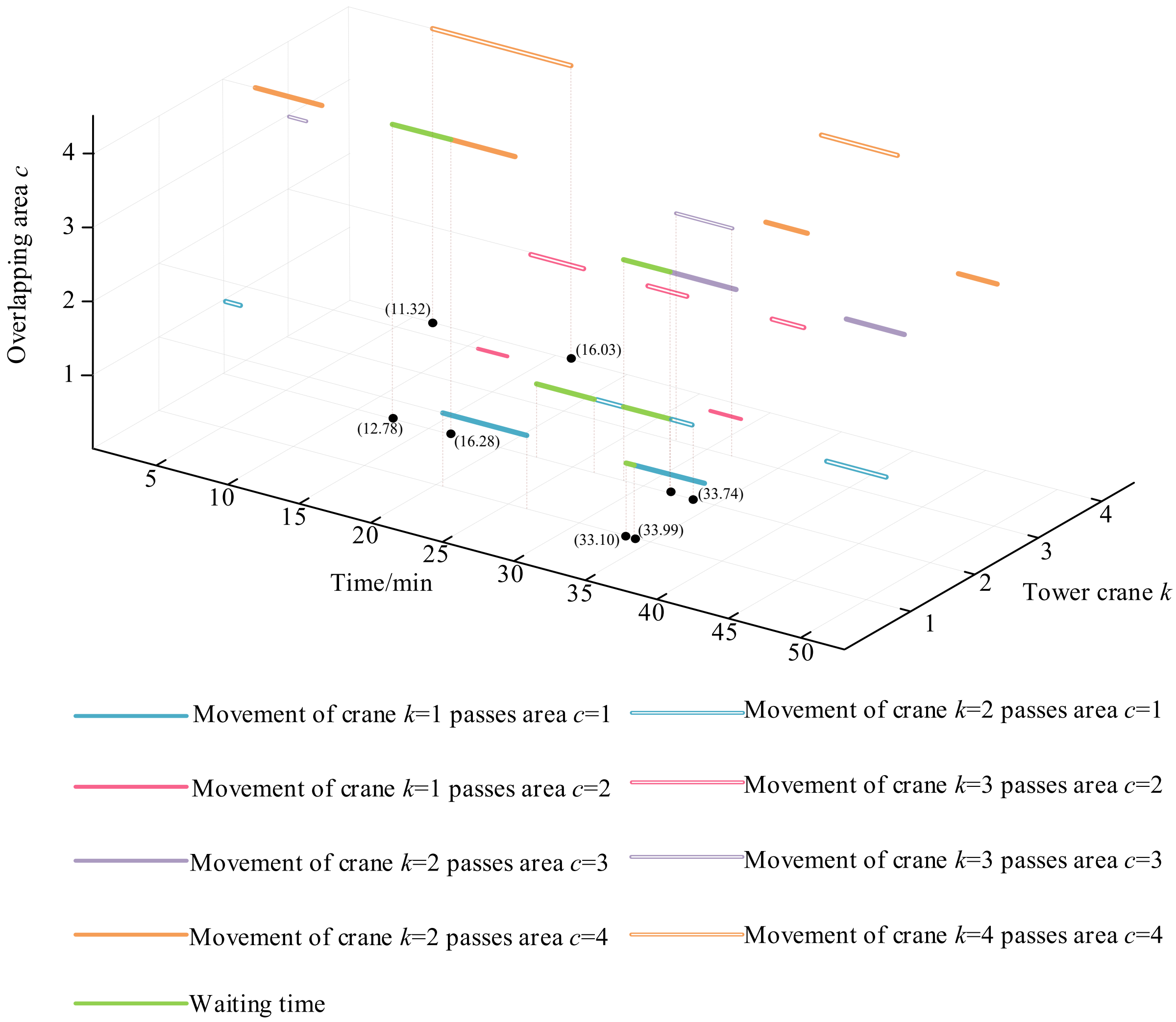

Fig. 6 Scenario of overlapping area occupied by the passive coordination method

The optimization model for the single CSSP [13] has been demonstrated to an effective method for identifying the optimum schedule for a single crane to complete lifting tasks within a minimum timeframe. The model relaxes the fixed pairs of supply and demand locations and the lifting sequences as variables. Table 11 details crane movements with minimum operation times (149.76 min) and costs (687.84 CNY). However, four collisions occurred during the crane movements. In Fig. 7, a solid line and a hollow line in the same color existing in the same period indicates an instance of simultaneous crane movements inside an overlapping area. For example, the tower crane at a location k=2 and the tower crane at the location k=4 entered the same overlapping area c=4 at 2.48 min and 3.00 min. This might trigger a potential collision. There were also two other collisions that might possibly have occurred in the overlapping area c=1 between the time 13.16 min and 18.89 min and in the area c=4 between the time 20.34 min and 26.40 min. Additionally, both of the tower cranes at locations k=1 and k=3 selected $D3$ as the destination location in their last movement and stayed inside the area c=2.

Table 11. Details of cranes movements optimized by the optimization model for a single tower crane

Crane location, k	Optimized sequence, s	Material request, r	Hook movement		Movement time, min	Movement cost, CNY*	Cumulative cost, CNY
			Start	End			
1	1	12	$D5$	$S2$	2.29	9.87	9.87
			$S2$	$D1$	4.82	34.92	44.79
	2	11	$D1$	$S1$	2.02	9.06	53.85
			$S1$	$D2$	3.75	28.50	82.35
	3	4	$D2$	$S1$	3.75	14.25	96.60
			$S1$	$D5$	5.10	36.60	133.2
	4	6	$D5$	$S2$	2.29	9.87	143.07
			$S2$	$D3$	5.02	36.12	179.19
2	1	8	$D2$	$S3$	3.59	13.77	13.77
			$S3$	$D7$	2.10	18.60	32.37
	2	7	$D7$	$S3$	2.10	9.30	41.67
			$S3$	$D3$	4.83	34.98	76.65
	3	15	$D3$	$S3$	4.83	17.49	94.14
			$S3$	$D6$	6.22	43.32	137.46
	4	1	$D6$	$S4$	4.82	17.46	154.92
			$S4$	$D8$	3.17	25.02	179.94
3	1	9	$D6$	$S6$	4.45	16.35	16.35
			$S6$	$D9$	2.76	22.56	38.91
	2	16	$D9$	$S5$	5.54	19.62	58.53
			$S5$	$D10$	1.50	15.00	73.53
	3	10	$D10$	$S5$	1.50	7.50	81.03
			$S5$	$D4$	2.85	23.10	104.13
	4	5	$D4$	$S5$	2.85	11.55	115.68
			$S5$	$D3$	4.19	31.14	146.82
4	1	14	$D11$	$S3$	4.19	15.57	15.57
			$S3$	$D11$	4.19	31.14	46.71
	2	2	$D11$	$S7$	1.67	8.01	54.72
			$S7$	$D14$	4.46	32.76	87.48
	3	3	$D14$	$S3$	5.82	20.46	107.94
			$S3$	$D12$	5.04	36.24	144.18

4	13	*D*12	*S*7	2.53	10.59	154.77
		*S*7	*D*13	3.52	27.12	181.89

*: Movement cost includes the operation cost and loading or unloading operation cost.

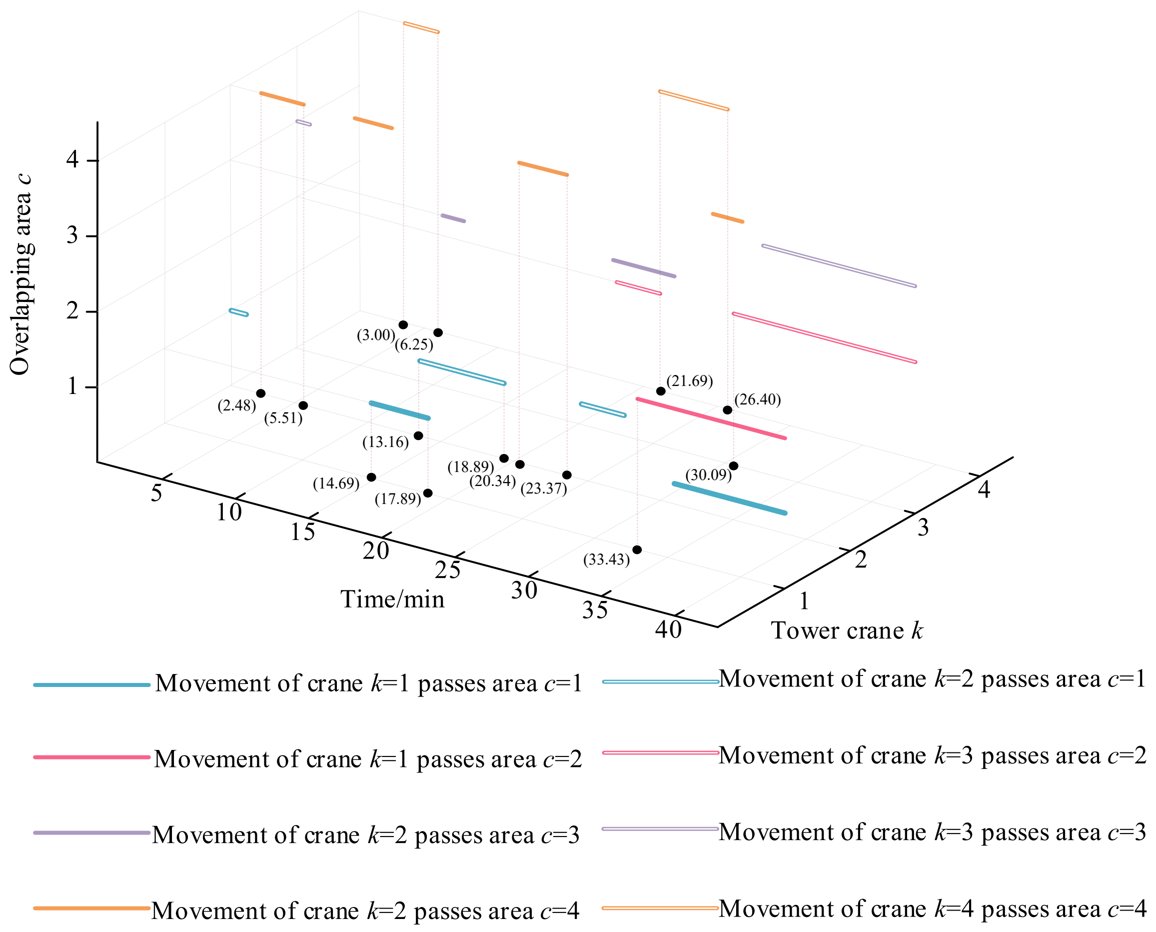

Fig. 7 Scenario of overlapping area occupied by tower cranes using optimized method for a single tower crane

Table 12 lists crane movements optimized by the proposed model. Crane movements passing through the overlapping areas are detailed in Table 13 and illustrated in Fig. 8. Obviously, these demonstrate that the model succeeds in preventing simultaneous movements inside any overlapping area. Total operation cost was reduced to 692.55 CNY (183.27+179.94+146.82+182.52). It takes 23.01 seconds to solve the problem using Gurobi 9.0 [45] with Intel Core i9-9900K @ 3.6 GHz and 32 GB RAM.

Table 12.

Details of crane movements optimized by the proposed model

Crane	Optimized	Material	Hook movement	Movement	Movement cost,	Cumulative cost,

location, *k*	sequence, *s*	request, *r*	Start	End	time, min	CNY*	CNY
1	1	6	*D*5	*S*2	2.29	9.87	9.87
			*S*2	*D*3	5.02	36.12	45.99
	2	4	D3	*S*1	5.11	18.33	64.32
			*S*1	*D*5	5.10	36.60	100.92
	3	12	*D*5	*S*2	2.29	9.87	110.79
			*S*2	*D*1	4.82	34.92	145.71
	4	11	*D*1	*S*1	2.02	9.06	154.77
			*S*1	*D*2	3.75	28.50	183.27
2	1	8	*D*2	*S*3	3.59	13.77	13.77
			*S*3	*D*7	2.10	18.60	32.37
	2	7	*D*7	*S*3	2.10	9.30	41.67
			*S*3	*D*3	4.83	34.98	76.65
	3	15	*D*3	*S*3	4.83	17.49	94.14
			*S*3	*D*6	6.22	43.32	137.46
	4	1	*D*6	*S*4	4.82	17.46	154.92
			*S*4	*D*8	3.17	25.02	179.94
3	1	9	*D*6	*S*6	4.45	16.35	16.35
			*S*6	*D*9	2.76	22.56	38.91
	2	10	*D*9	*S*5	5.54	19.62	58.53
			*S*5	*D*4	2.85	23.10	81.63
	3	16	*D*4	*S*5	2.85	11.55	93.18
			*S*5	*D*10	1.50	15.00	108.18
	4	5	*D*10	*S*5	1.50	7.50	115.68
			*S*5	*D*3	4.19	31.14	146.82
4	1	13	*D*11	*S*7	1.67	8.01	8.01
			*S*7	*D*13	3.52	27.12	35.13
	2	3	*D*13	*S*3	6.04	21.12	56.25
			*S*3	*D*12	5.04	36.24	92.49
	3	14	*D*12	*S*3	5.04	18.12	110.61
			*S*3	*D*11	4.19	31.14	141.75
	4	2	*D*11	*S*7	1.67	8.01	149.76
			*S*7	*D*14	4.46	32.76	182.52

*: Movement cost includes the operation cost and loading or unloading operation cost.

Table 13.

Details of cranes movements passing overlapping areas optimized by the proposed model

Overlapping area, *c*	Tower crane setup location, *k*	Movement path	Enter time, *TI* (cumulative time, min)	Leave time, *TO* (cumulative time, min)
1	2	*D*2→*S*3	0	*p*2(1.03)
	1	*S*2→*D*3→*S*1	*p*1(7.78)	*p*2(11.68)
	2	*S*3→*D*3→*S*3	*p*2(13.16)	*p*2(18.89)
	2	*S*3→*D*6	*p*2(24.82)	*p*1(27.54)
	1	*S*1→*D*2	*p*2(36.22)	-*
2	1	*S*2→*D*3→*S*1	*p*4(5.68)	*p*3(9.72)
	3	*S*5→*D*4→*S*5	*p*4(17.38)	*p*4(20.64)
	3	*S*5→*D*3	*p*4(30.09)	-

3	3	*D6*→*S6*	0	*p*5(1.21)
	2	*S3*→*D3*→*S3*	*p*6(15.14)	*p*6(16.91)
	2	*S3*→*D6*→*S4*	*p*6(26.80)	*p*5(30.88)
	3	*S5*→*D3*	*p*6(32.23)	-
4	2	*D2*→*S3*→*D7*	*p*8(2.48)	*p*8(5.51)
	2	*D7*→*S3*→*D3*	*p*8(8.68)	*p*8(11.72)
	4	*D13*→*S3*→*D12*	*p*8(12.04)	*p*8(15.31)
	2	*D3*→*S3*→*D6*	*p*8(20.33)	*p*8(23.37)
	4	*D12*→*S3*→*D11*	*p*8(24.13)	*p*8(27.40)
	2	*D6*→*S4*→*D8*	*p*7(33.50)	*p*7(36.32)

*The tower crane stayed inside the overlapping area, and the time *TO* is set as an arbitrary large number.

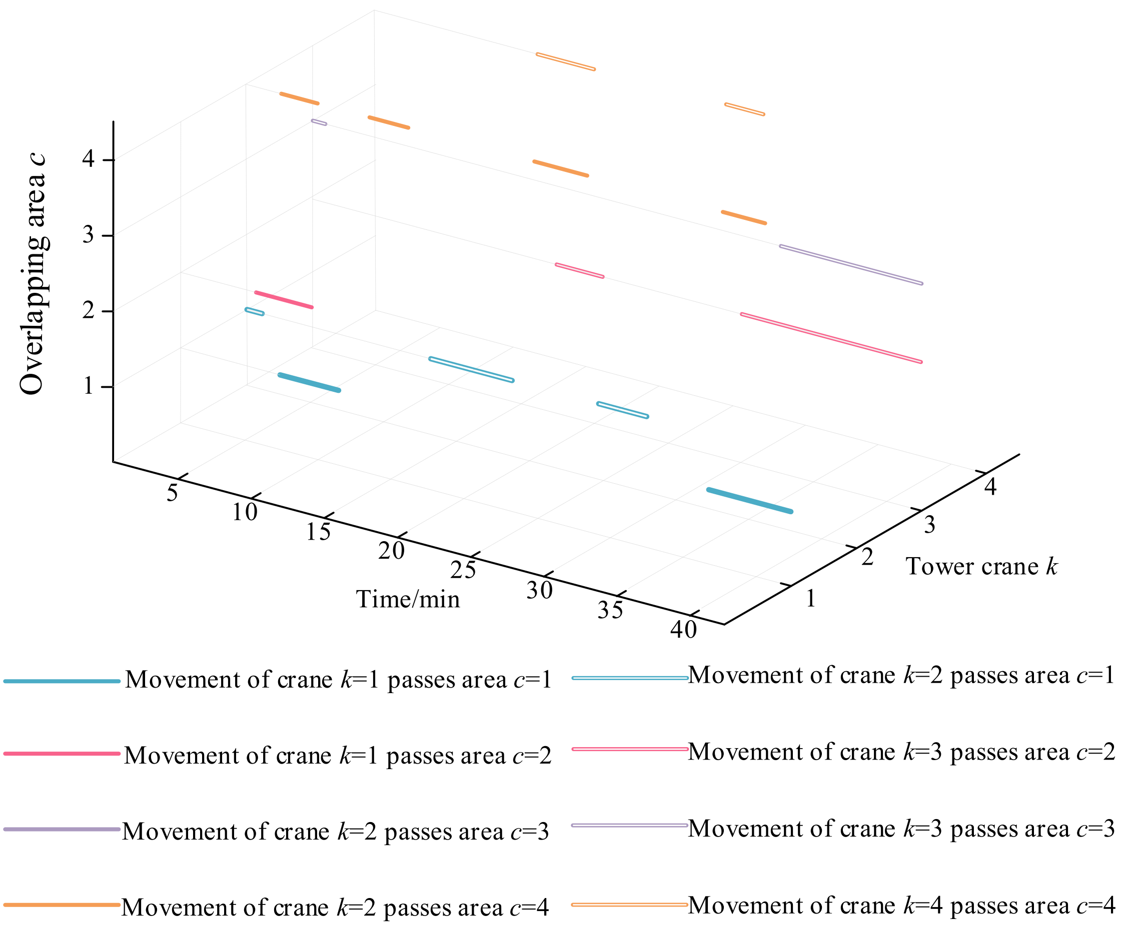

Fig. 8 Scenario of overlapping area occupied by tower cranes using optimized method for multiple tower cranes

Table 14 compares the operation costs of four tower cranes based on different scheduling strategies. Taking the cost optimized by the proposed model as the reference, the results show that the passive coordination method increased 18.07%. Although the model for CSSP saved 0.68% of the total cost, four collisions were triggered following the schedule optimized by the model. To demonstrate the effectiveness of the proposed model, the number of requests is increased from 16 to 32. Detailed in Table 15, the cost difference optimized by the two models ranges between 0.6% and 1.01%. However, the computation time of the proposed model rises exponentially from 23.01 seconds to 2,599.79 seconds.

Table 14.

Comparison of operation costs using different service strategies

Scheduling method	The passive coordination method	The model for CSSP	The model for MCSSP
Total operation cost (CNY)	817.71	687.84	692.55
The difference of the operation cost	18.07%	-0.68%	-

Table 15.

Comparisons of the results optimized by the models for CSSP and MCSSP with different numbers of requests

Number of requests	CSSP		MCSSP		Gap
	Cost, CNY	Computation time, second	Cost, CNY	Computation time, second	
16	687.84	20.11	692.55	23.01	0.68%
20	861.97	162.16	870.71	84.62	1.01%
24	1047.45	268.51	1,055.07	213.12	0.73%
28	1,172.39	299.87	1,179.37	438.68	0.60%
32	1,373.78	3,156.55	1,382.54	2,599.79	0.64%

The tower crane scheduling problem is an NP-hard problem [50, 58]. With the rise of the variable number, the nature of the problem will result in exponentially increased computation time. To obtain the absolute optimal solution as the reference to evaluate the quality of other heuristic algorithms, this research proposed the MILP model, solved using Gurobi. The absolute optimal solution always requires a large amount of time. To speed up the solving process, the variable tolerance in the Gurobi solver was set from 10^{-5} to 10^{-2} (i.e., if a variable is between 0.99 and 1.01, it will be transferred to be the integer 1). Practically, to obtain a near-optimal solution in a limited time, the optimization process can be terminated by setting the optimality gap between the lower and upper objective bound or the upper CPU processing time. As shown in Table 16, by setting the optimality gap as 5% and the upper computation time as 2000 seconds, the computation time can be significantly decreased from 12.9% to 78.6% while the optimality gap remains between 0.73% and 4.04%.

Table 16.

Comparisons of the results optimized by the models on two parameter settings with different numbers of requests

Number of requests	Absolute optimal solution*		Near-optimal solution**		Gap
	Cost, CNY	Computation time, second	Cost, CNY	Computation time, second	
16	692.56	23.01	697.63	17.32	0.73%
20	870.71	84.62	884.09	55.89	1.54%
24	1055.07	213.12	1079.67	185.65	2.33%
28	1179.37	438.68	1226.96	244.62	4.04%
32	1382.54	2599.79	1409.23	556.01	1.93%

*: Variable tolerance=10^{-2}

**: Variable tolerance=10^{-2} & Gap=5% & Time limit=2000s

The dynamic supply selection system [3] was also applied in the numerical example. In the system, each supply location was set to provide all the materials. The lifting sequence followed the same priority of the 16 requests determined by the crane signal man. Table 17 shows the operation cost and the crane movement routes optimized by the two models. The comparison shows that the dynamic supply selection system consumed 647.50 CNY of the operation cost, which is 6.54% more than the cost optimized by the proposed model.

Table 17.
Details of hook movements of the tower cranes optimized by the dynamic supply selection system and proposed model

Method	Tower crane, k	Crane movement routes	Total cost (CNY)
Dynamic supply selection system	1	$D5\to S2\to D5\to S2\to D3\to S1\to D2\to S1\to D1$	647.50
	2	$D2\to S4\to D8\to S3\to D3\to S3\to D7\to S4\to D6$	
	3	$D6\to S5\to D3\to S6\to D9\to S5\to D4\to S5\to D10$	
	4	$D11\to S7\to D14\to S7\to D12\to S7\to D13\to S7\to D11$	
Proposed method	1	$D5\to S2\to D5\to S2\to D3\to S1\to D1\to S1\to D3$	607.78
	2	$D2\to S3\to D2\to S3\to D7\to S4\to D8\to S4\to D6$	
	3	$D6\to S5\to D4\to S5\to D10\to S5\to D3\to S6\to D9$	
	4	$D11\to S7\to D13\to S7\to D12\to S7\to D11\to S7\to D14$	

6. Conclusions

This study aimed to improve the operation efficiency of multiple tower cranes by minimizing energy costs and eliminating movement interference in overlapping areas. The Multiple Crane Sequence Service Problem (MCSSP) is formulated as a Mixed Integer Linear Programming (MILP) problem. Various binary variables and linear governing constraints are introduced to model the crane operations and avoid simultaneous jib movements inside an overlapping area. To prevent potential collisions, the model prevents simultaneous crane movements in an overlapping area efficiently and automatically by 1) distributing lifting requests in overlapping areas to the appropriate tower cranes; 2) selecting the appropriate supply location to serve each lifting request; and 3) arranging the lifting sequence of a tower crane to complete the requests. The optimization problem is solved by using Gurobi^{TM} 9.0. The results reveal that the proposed model can effectively balance safety with material transportation efficiency.

However, the MCSSP has been demonstrated as an NP-hard problem, and the proposed model is very time-consuming. For complicated construction sites with multiple tower cranes, the model must be improved by introducing more efficient constraints or more effective optimization algorithms (e.g., a parallel Genetic Algorithm). The model's estimation of hook movement time is inaccurate. Through combination with a long-term position tracking technique, the present model might be improved and extended by the provision of accurate hook movement data. Large data collection and analysis can then be employed to reduce the impact of uncertainties during the material transportation to achieve just-in-time delivery.

Acknowledgements

This work was supported by the Science & Technology Fund of Beijing Education Committee (No: KM202110005019).

References

[1] S. Hwang, Ultra-wide band technology experiments for real-time prevention of tower crane collisions, Automation in Construction 22 (2012) 545-553, https://doi.org/10.1016/ j.autcon.2011.11.015.

[2] J. Irizarry, E.P. Karan, Optimization location of tower cranes on construction sites through GIS and BIM integration, Journal of Information Technology in Construction 17 (2012) 351-366, https://www.itcon.org/papers/2012_23.content.06091.pdf.

[3] A. Khodabandelu, J. Park, C. Arteaga, Crane operation planning in overlapping areas through dynamic supply selection, Automation in Construction 117 (2020) 103253, https://doi.org/10.1016/j.autcon.2020. 103253.

[4] M.A. Hattab, E. Zankoul, M. Braakat, F. Hamzeh, Crane overlap and operational flexibility: balancing utilization, duration, and safety, Construction Innovation 18 (1) (2018) 43-63, https://doi.org/10.1108/CI-11-2016-0062.

[5] Z. Zhang, W. Pan, Lift planning and optimization in construction: A thirty-year review, Automation in Construction 118 (2020) 103271, https://doi.org/10.1016/j.autcon.2020. 103271.

[6] X. Li, H. Chi, P. Wu, G.Q. Shen, Smart work packaging-enabled constraint-free path re-planning for tower crane in prefabricated products assembly process, Advanced Engineering Informatics 43 (2020) 101008, https://doi.org/10.1016/ j.aei.2019.101008.

[7] C. Zhang, A. Hammad, S. Rodriguez, Crane pose estimation using UWB real-time location system, Journal of Computing in Civil Engineering 26 (5) (2012) 625-637, https://doi.org/10.1061/(ASCE)CP.1943-5487.0000172.

[8] G. Lee, J. Cho, S. Ham, T. Lee, G. Lee, S. Yun, H.J. Yang, A BIM- and sensor-based tower crane navigation system for blind lifts, Automation in Construction 26 (2012) 1-10, https://doi.org/10.1016/j.autcon.2012.05.002.

[9] H. Li, G. Chan, M. Skitmore, Integrating real time positioning systems to improve blind lifting and loading crane operations, Construction Management and Economics 31 (6) (2013) 596-605, https://doi.org/10.1080/01446193.2012.756144.

[10] Y. Fang, Y. K. Cho, J. Chen, A framework for real-time pro-active safety assistance for mobile crane lifting operations, Automation in Construction 72 (2016) 367-379, https://doi.org/10.1016/j.autcon.2016.08.025.

[11] G. Lee, H.H. Kim, C.J. Lee, S.I. Ham, S.H. Yun, H. Cho, B.K. Kim, G.T. Kim, K. Kim, A laser-technology-based lifting-path tracking system for a robotic tower crane, Automation in Construction 18 (7) (2009) 865-874, https://doi.org/10.1016/ j.autcon.2009.03.011.

[12] D.D. Liu, W.S. Lu, Y.H. Niu, F. Xue, K. Chen, Bridging the cyber and physical systems for better construction: A case study of construction machinery monitoring and utilization, International Symposium on Advancement of Construction Management and Real Estate. Springer, Singapore, 2018, https://doi.org/10.1007/978-981-10-6190-5_35.

[13] C. Huang, C.K. Wong, Optimization of crane setup location and servicing schedule for urgent material requests with non-homogeneous and non-fixed material supply, Automation in Construction 89 (2018) 183-198, https://doi.org/10.1016/j.autcon.2018.01.015.

[14] M.A. Hattab, E. Zankoul, F.R. Hamzeh, Near-real-time optimization of overlapping tower crane operations: a model and case study, Journal of Computing in Civil Engineering 31 (4) (2017) 05017001, https://doi.org/10.1061/(ASCE)CP.1943-5487.0000666.

[15] C. M. Tam, Thomas K.L. Tong, Wilson K.W. Chan, Genetic algorithm for optimizing supply locations around tower crane, Journal of Construction Engineering and Management 127 (4) (2001) 315-321, https://doi.org/10.1061/(ASCE)0733-9364(2001)127:4(315)

[16] M.A. Abdelmegid, K.M. Shawki, H. Abdel-Khalek, GA optimization model for solving tower crane location problem in construction sites, Alexandria Engineering Journal 54 (3) (2015) 519-526, https://doi.org/10.1016/j.aej.2015.05.011.

[17] M. Marzouk, A. Abubakr, Decision support for tower crane selection with building information models and genetic algorithms, Automation in Construction 61 (2016) 1-15, https://doi.org/10.1016/j.autcon. 2015.09.008.

[18] C. Huang, C. K. Wong, C. M. Tam, Optimization of tower crane and material supply locations in a high-rise building site by mixed-integer linear programming, Automation in Construction 20 (5) (2011) 571-580, https://doi.org/10.1016/j.autcon.2010.11.023.

[19] Z.S.M. Nadoushani, A.W.A. Hammad, A. Akbarnezhad, Location optimization of tower crane and allocation of material supply points in a construction site considering operating and

rental costs, Journal of Construction Engineering and Management 143 (1) (2017) 04016089, https://doi.org/10.1061/(ASCE) CO.1943-7862.0001215.

[20] D. Briskorn, M. Dienstknecht, Mixed-integer programming models for tower crane selection and positioning with respect to mutual interference, European Journal of Operational Research 273 (1) (2019) 160-174, https://doi.org/10.1016/ j.ejor.2018.07.033.

[21] Y. Ji, F. Leite, Optimized planning approach for multiple tower cranes and material supply points using mixed-integer programming, Journal of Construction Engineering and Management 146 (3) (2020) 04020007, https://doi.org/10.1061/(ASCE)CO.1943-7862. 0001781.

[22] J. K. W. Yeoh, D. K. H. Chua, Optimizing Crane Selection and Location for Multistage Construction Using a Four-Dimensional Set Cover Approach, Journal of Construction Engineering and Management 143 (8) (2017) 04017029, https://doi.org/10.1061/(ASCE) CO.1943-7862.0001318.

[23] A. Younes, M. Marzouk, Tower cranes layout planning using agent-based simulation considering activity conflicts, Automation in Construction, 93 (2018) 348-360, https://doi.org/10.1016/j.autcon.2018.05.030.

[24] K. Wu, B.G. de Soto, F. Zhang, Spatio-temporal planning for tower cranes in construction projects with simulated annealing, Automation in Construction 111 (2020) 103060, https://doi.org/10.1016/j.autcon.2018.05.030.

[25] Y. Ji, F. Leite, Automated tower crane planning: Leveraging 4-dimensional BIM and rule-based checking, Automation in Construction 93 (2018) 78-90, https://doi.org/10.1016/j.autcon.2018.05.003.

[26] Y. Sugimoto, H. Seki, T. Samo, N. Nakamitsu, 4D CAD-based evaluation system for crane deployment plans in construction of nuclear power plants, Automation in Construction 71 (2016) 87-98, https://doi.org/10.1016/j.autcon.2016.04.004.

[27] S.C. Kang, E. Miranda, Planning and visualization for automated robotic crane erection processes in construction, Automation in Construction 15 (4) (2006) 398 – 414, https://doi.org/10.1016/j.autcon.2005.06.008.

[28] S.C. Kang, E. Miranda, Numerical methods to simulate and visualize detailed crane activities, Computer-Aided Civil and Infrastructure Engineering 24 (3) (2009) 169 – 185, https://doi.org/10.1111/j.1467-8667.2008.00579.x.

[29] P. L. Sivakumar, K. Varghese, N. R. Babu. Automated path planning of cooperative crane lifts using heuristic search, Journal of Computing in Civil Engineering 17 (3) (2003) 197-207, https://doi.org/10.1061/(ASCE)0887-3801(2003) 17:3(197).

[30] P. Cai, I. Chandrasekaran, Y. Cai, , J. Zheng, Y. Gong, T. S. Lim, P. Wong, Collision detection using axis aligned bounding boxes, Simulation, Serious Games and Their Applications, Springer, 2013, 1-14.

[31] S. Dutta, Y. Cai, L. Huang, J. Zheng, Automatic re-planning of lifting paths for robotized tower cranes in dynamic BIM environments, Automation in Construction 110 (2020) 110: 102998, https://doi.org/10.1016/j.autcon.2019.102998.

[32] J. W. Chang, W. Wang, M. S. Kim, Efficient collision detection using a dual OBB-sphere bounding volume hierarchy, Computer-Aided Design 42 (1) (2010) 50-57, https://doi.org/10.1016/j.cad.2009.04.010.

[33] M.S.A.D. Ali, N.R. Babu, K. Varghese, Collision free path planning of cooperative crane manipulators using genetic algorithm, Journal of Computing in Civil Engineering 19 (2) (2005) 182-193, https://doi.org/10.1061/(ASCE)0887-3801 (2005)19:2(182).

[34] C. Zhang, A. Hammad, Improving lifting motion planning and re-planning of cranes with consideration for safety and efficiency, Advanced Engineering Informatics 26 (2) (2012) 396-410, https://doi.org/10.1016/j.aei.2012.01.003.

[35] Y.C. Chang, W.H. Hung, S.C. Kang, A fast path planning method for single and dual crane erections, Automation in Construction 22 (2012) 468-480, https://doi.org/10.1016/j.autcon.2011.11.006.

[36] H.R. Reddy, K. Varghese, Automated path planning for mobile crane lifts, Computer-Aided Civil and Infrastructure Engineering 17 (6) (2002) 439–448, https://doi.org/10.1111/0885-9507.00005.

[37] P. Cai, Y. Cai, I. Chandrasekaran, J. Zheng, Parallel genetic algorithm based automatic path planning for crane lifting in complex environments, Automation in Construction 62 (2016) 133-147, https://doi.org/10.1016/j.autcon.2015.09.007.

[38] H. Kawai, Y. Kim, Y. Choi, Measurement of a container crane spreader under bad weather conditions by image restoration, IEEE Transaction on Instrumentation and Measurement 61 (1) (2012) 35-42, https://doi.org/10.1109/TIM.2011.2161830.

[39] S. Chi, C.H. Caldas, Automated object identification using optical video cameras on construction sites, Computer-Aided Civil and Infrastructure Engineering 26 (2011) 368–380, https://doi.org/10.1111/j.1467-8667.2010.00690.x.

[40] Z. Cai, M. Saberian, N. Vasconcelos, Learning complexity-aware cascades for deep pedestrian detection, The IEEE International Conference on Computer Vision (ICCV), IEEE, Santiago, 2015, https://doi.org/10.1109/ICCV.2015.384

[41] T. Sutjaritvorakul, A. Vierling, J. Pawlak, K. Berns, Simulation platform for crane visibility safety assistance, Advances in Service and Industrial Robotics, Springer, Cham, 2020, https://doi.org/10.1007/978-3-030-48989-2_3.

[42] J. Kim, S. Chi, M. Choi, Sequential pattern learning of visual features and operation cycles for vision-based action recognition of earthmoving excavators. International Conference on Computing in Civil Engineering, ASCE, Atlanta, 2019, https://doi.org/10.1061/9780784482438.038.

[43] J. Bruce, M. Veloso, Real-time randomized path planning for robot navigation, International Conference on Intelligent Robots and Systems, IEEE, Lausanne, 2002, https://doi.org/10.1007/978-3-540-45135-8_23.

[44] D. Ferguson, N. Kalra, A. Stentz, Replanning with RRTs, International Conference on Robotics and Automation, IEEE, Orlando, 2006, https://doi.org/10.1109/robot.2006.1641879.

[45] Y. Wang, I.P.W. Sillitoe, D.J. Mulvaney, Mobile robot path planning in dynamic environments, International Conference on Robotics and Automation, IEEE, Roma, 2007, https://doi.org/10.1109/robot.2007.363767.

[46] H. Miao, Y. C. Tian, Dynamic robot path planning using an enhanced simulated annealing approach, Applied Mathematics and Computation 222 (2013) 420 – 437, https://doi.org/10.1016/j.amc.2013.07.022.

[47] Y. Wu, N. Sun, H. Chen, Y. Fang, Adaptive output feedback control for 5-DOF varying-cable-length tower cranes with cargo mass estimation, IEEE Transactions on Industrial Informatics 17 (4) (2021) 2453 - 2464, https://doi.org/10.1109/TII.2020.3006179.

[48] T. Yang, N. Sun, Y. Fang, Adaptive Fuzzy Control for a Class of MIMO Underactuated Systems With Plant Uncertainties and Actuator Deadzones: Design and Experiments. IEEE Transactions on Cybernetics (2021) 1-14, https://doi.org/10.1109/TCYB.2021. 3050475.

[49] T. Yang, N. Sun, H. Chen, Y. Fang, Observer-based nonlinear control for tower cranes suffering from uncertain friction and actuator constraints with experimental verification. IEEE Transactions on Industrial Electronics (2020), https://doi.org/10.1109/TIE. 2020.2992972.

[50] A. Zavichi, K. Madani, P. Xanthopoulos, A.A. Oloufa, Enhanced crane operations in construction using service request optimization, Automation in Construction 47 (2014) 69-77, https://doi.org/10.1016/j.autcon.2014.07.011.

[51] A. Tork, A real-time crane service scheduling decision support system (css-dss) for Cconstruction tower cranes, Ph.D. Thesis, College of Engineering and Computer Science, University of Central Florida, 2013, http://purl.fcla.edu/fcla/etd/CFE0005078.

[52] S. Monghasemi, M.R. Nikoo, J. Adamowski, Sequential ordering of crane service requests considering the pending times of the requests: An approach based on game theory and optimization techniques, Automation in Construction 70 (2016) 62-76, https://doi.org/10.1016/j.autcon.2016.06.006.

[53] S. Hougardy, M. Wilde, On the nearest neighbor rule for the metric traveling salesman problem, Discrete Applied Mathematics 195 (2015) 101-103, https://doi.org/10.1016/j.dam.2014.03.012.

[54] L. Du, R. He, Combining Nearest Neighbor Search with Tabu Search for Large-Scale Vehicle Routing Problem, Physics Procedia 25 (2012) 1536-1546, https://doi.org/10.1016/j.phpro.2012.03.273.

[55] W. Ren, Z. Wu, Real-time anticollision system for mobile cranes during lift operations, Journal of Computing in Civil Engineering 29 (6) (2015) 04014100, https://doi.org/10.1061/(ASCE)CP.1943-5487.0000438.

[56] Y. Li, C. Liu, Integrating field data and 3D simulation for tower crane activity monitoring and alarming, Automation in Construction 27 (2012) 111-119, https://doi.org/10.1016/j.autcon.2012.05.003.

[57] Y. Zhu, A. Lim, Crane scheduling with non-crossing constraint, Journal of the Operational Research Society 57 (12) (2006) 1464-1471, https://doi.org/10.1057/ palgrave.jors. 2602110.

[58] H. Tarhini, B. Maddah, F. Hamzeh. The Traveling Salesman Puts-on a Hard Hat-Tower Crane Scheduling in Construction Projects, European Journal of Operational Research (2020) https://doi.org/10.1016/j.ejor.2020.10.029.

[59] Gurobi Optimization LLC, (2020), Gurobi optimizer reference manual. URL: http://www.gurobi.com.

[60] P. Zhang, F.C. Harris, P.O. Olomolaiye, A computer‐based model for optimizing the location of a single tower crane, Building research and information 24 (2) (1996) 113-123, https://doi.org/10.1080/09613219608727511.

[61] P. Cai, I. Chandrasekaran, J. Zheng, Y. Cai, Automatic path planning for dual-crane lifting in complex environments using a prioritized multiobjective PGA, IEEE Transactions on Industrial Informatics 14 (3) (2017) 829-845, DOI: 10.1109/TII.2017.2715835.

Appendix I

Algorithm 1 Pseudo-code of the process to calculate the time for a crane to enter or leave an overlapping area

```
for each scheduling in all possible combinations do
    for each single tower crane route in scheduling do
        if a crane movement passes through an overlapping area then
            if the initial hook location is inside the overlapping area then
                TI ← 0 (Eq. 31-a)
                TO ← TI + T (the movement time from the start location to the selected intersection point) (Eq. 33-a)
            else if the start location is inside an overlapping area in the rest sequences then
                TI ← M (an arbitrary large number) (Eq. 31-b and Eq.31-c)
                TO ←TI + T (the movement time from entering the area to leaving the area) (Eq. 33-c and Eq. 33-d)
            else the start location is outside the overlapping area in the rest sequences then
                TI ← ST + T (the movement time from the start location to the selected intersection point) (Eq. 31-d and Eq.31-e)
                if the destination is inside the overlapping area in the last sequence then
                    TO ← TI + M (An arbitrary large number) (Eq. 33-b)
                else if the destination is inside an overlapping area in the rest sequences then
                    TO ← TI + T(the movement time from entering the area to leaving the area) (Eq. 33-c and 33-d)
                else the destination is outside an overlapping area in the rest sequences then
                    TO ← TI + T(the movement time passes the entire overlapping area) (Eq. 33-e)
                end if
            end if
        else a crane does not pass any overlapping area then
            TI ← M (An arbitrary large number) (Eq. 31-f and Eq. 31-g), TO ← M (Eq. 33-f)
        end if
    end for
end for
```